

## Table of Contents

Statement of the problem studied .....	1
Summary of the most important results .....	2
Bibliography .....	3
Appendixes	
1. Measurements of Electrothermal-Plasma Ignition of Solid Propellants.....	4
2. Optical Measurements of the Interaction Between Electrothermal-Plasmas and Solid Propellants.....	15
3. Spectroscopic Measurements During an Electrothermal Plasma-JA2 Solid Propellant Interaction .....	25

Report Documentation Page				Form Approved OMB No. 0704-0188	
Public reporting burden for the collection of information is estimated to average 1 hour per response, including the time for reviewing instructions, searching existing data sources, gathering and maintaining the data needed, and completing and reviewing the collection of information. Send comments regarding this burden estimate or any other aspect of this collection of information, including suggestions for reducing this burden, to Washington Headquarters Services, Directorate for Information Operations and Reports, 1215 Jefferson Davis Highway, Suite 1204, Arlington VA 22202-4302. Respondents should be aware that notwithstanding any other provision of law, no person shall be subject to a penalty for failing to comply with a collection of information if it does not display a currently valid OMB control number.					
1. REPORT DATE <b>31 JUL 2005</b>		2. REPORT TYPE <b>N/A</b>		3. DATES COVERED <b>-</b>	
4. TITLE AND SUBTITLE <b>Experimental Investigation of the Interaction of Electrothermal Plasmas With Solid Propellants</b>				5a. CONTRACT NUMBER	
				5b. GRANT NUMBER	
				5c. PROGRAM ELEMENT NUMBER	
6. AUTHOR(S)				5d. PROJECT NUMBER	
				5e. TASK NUMBER	
				5f. WORK UNIT NUMBER	
7. PERFORMING ORGANIZATION NAME(S) AND ADDRESS(ES) <b>University of Texas - Austin Office of Sponsored Projects 101 E. 27th Street Austin, TX 78712</b>				8. PERFORMING ORGANIZATION REPORT NUMBER	
9. SPONSORING/MONITORING AGENCY NAME(S) AND ADDRESS(ES)				10. SPONSOR/MONITOR'S ACRONYM(S)	
				11. SPONSOR/MONITOR'S REPORT NUMBER(S)	
12. DISTRIBUTION/AVAILABILITY STATEMENT <b>Approved for public release, distribution unlimited</b>					
13. SUPPLEMENTARY NOTES <b>The original document contains color images.</b>					
14. ABSTRACT					
15. SUBJECT TERMS					
16. SECURITY CLASSIFICATION OF:			17. LIMITATION OF ABSTRACT <b>SAR</b>	18. NUMBER OF PAGES <b>36</b>	19a. NAME OF RESPONSIBLE PERSON
a. REPORT <b>unclassified</b>	b. ABSTRACT <b>unclassified</b>	c. THIS PAGE <b>unclassified</b>			

## Statement of the problem studied

Studies of propellant charges ignited by plasma discharges have shown that this technique has significant advantages over conventional (primer) ignition.<sup>1-8</sup> It has been shown that ignition delay and jitter were substantially reduced, and temperature compensation achieved, with a plasma energy input that was substantially smaller than the energy required to heat the propellant bed to the reference condition. However, the mechanism that is responsible for the improved performance is unknown. The plasma could function merely as an improved thermal source since it has a very high temperature compared to conventional combustion products. It could function as a radiant source that distributes the energy into the propellant bed more uniformly and rapidly than simple flame spread. Additionally, the plasma could provide a source of highly reactive species, not present in flames, which promote rapid and reliable ignition. In some configurations, plasma jets issuing into the propellant beds may penetrate more effectively than combustion products from a primer, and thus give a more distributed ignition. It is also possible that the blast wave accompanying the plasma discharge causes microfractures in the propellant grains that increases the burning surface area sufficiently to provide temperature compensation, though it seems hard to reconcile the observed repeatability of the process with known mechanisms of microfracture.

A combination of several of these mechanisms might also contribute to the observed performance improvement. An improved fundamental understanding of the interaction will help the Army design better initiators that tailor the plasma to the propellant, and thus reducing energy required or enhancing gun performance. For example, it may be possible to achieve the observed temperature compensation with a much smaller energy input than is currently needed, which would reduce the size of the power source required. Furthermore, because of the current lack of understanding, one cannot rule out the possibility that the plasma is interacting with only a minor component of the propellant charge, and thus plasma igniters could fail because of minor changes in propellant composition.

Owing to the complexity of the physical processes involved in plasma-induced ignition, achieving an understanding of the fundamental physics will likely be achieved only through computational/theoretical approaches aided by experimental data. The focus of the work was an experimental study of electrothermal-chemical (ETC) plasmas and their interaction with a representative solid propellant (JA-2). The objective was to obtain experimental data that would help validate models of the mechanisms that lead to rapid, repeatable ignition of propellant charges and which permit temperature compensation of the gun charge. This knowledge is essential if the Army is to field plasma initiators.

## Summary of the most important results

Heat flux measurements were made with a heat flux sensor along the axis of the plasma-jet. Measurements were made with and without a fused silica flat covering the sensor to enable the measurement of radiative and total heat flux, respectively. The peak total heat flux from the plasma to a surface was in excess of  $5 \text{ kW/cm}^2$  at a distance of 50 mm from the capillary exit. The peak radiant flux at this location was about  $2.5 \text{ kW/cm}^2$ , showing that the radiative heat flux is a substantial fraction of the total heat flux. Peak heating tended to occur at about 400  $\mu\text{s}$  well after the plasma luminosity had dissipated.

Experiments employing planar laser-induced fluorescence (PLIF) of atomic copper in the plasma showed that the very large background luminosity of the plasma greatly limits the quality of the measurements. The high luminosity necessitated the use of two-cameras to enable single-shot background subtraction.

The 3.1 kJ plasma impinging on JA-2 propellant disks in open-air experiments did not lead to ignition, but the propellant disks ignited when the plasma was impinged on them in closed chamber experiments. This demonstrated that pressurization due to confinement is critical to ignition. The formation of fine particulates due to condensation of the plasma significantly hinders the use of optical diagnostics in closed chamber experiments.

In order to study the initiation processes leading to ignition JA-2 discs in air were exposed to only the radiation from a confined 3.1 kJ electrothermal plasma discharge. The reactions induced by the plasma radiation in the propellant produce decomposition products as well as particulates that escape the propellant and propagate away from the surface. Nitric oxide (NO) is a common double base propellant decomposition product. Planar laser induced fluorescence (PLIF) measurements of NO were made in the gas bordering the propellant during the 600  $\mu\text{s}$  plasma discharge. Planar laser scattering (PLS) measurements were also conducted on the particulates in the same region. No reaction products were observed for the first 100  $\mu\text{s}$  after the discharge was triggered. Clouds of NO and scattering particles appeared at the propellant surface after this 100  $\mu\text{s}$  delay and expanded and propagated away from the surface as the discharge progressed. The clouds appeared in two varieties, the more prevalent type characterized by lower fluorescence and scattering signals with a globular structure, and the rarer type characterized by a larger size, very bright scattering signals, brighter fluorescence, and a smoother surface.

Further details of the results obtained during this work are given in the appendix which has reprints of three papers<sup>9-11</sup> published during the course of this work.

## Bibliography

1. Shaw, R.W., Mann, D.M., Anderson, W.R., White, K., Nusca, M.J. and Powell, J., "Army Plasma/Propellant Interaction Workshop – U.S. Army Research Office 17-18 November 1998," Report No. ARL-SR-83, November 1999.
2. Oberle, W., White, K. and Powell, J., "JANNAF Combustion Subcommittee Workshop: Plasma / Propellant Interaction and Propellant Temperature Sensitivity Reduction Using Electrothermal-Chemical (ETC) Propulsion Concepts." Report ARL-TR-1579, U.S. Army Research Laboratory, Aberdeen Proving Ground, MD, December 1997.
3. Edwards, C., Bourham, M. and Gilligan, J., "Experimental studies of the plasma-propellant interface for electrothermal-chemical launchers," *IEEE Transactions on Magnetics* **31** (1), p. 404-409, 1995.
4. Greig, J. R., Earnhart, J. R., Winsor, N., McElroy, H. A., Juhasz, A. A., Wren, G. P., and Morrison, W. F., "Investigation of Plasma Augmented Solid Propellant Interior Ballistic Processes," *IEEE Transactions on Magnetics* **29** (1), 1993, pp. 555-560.
5. Woodley, C. R., "A Parametric Study for an Electrothermal-Chemical Artillery Weapon," *IEEE Transactions on Magnetics* **29** (1), 1993, pp. 625-630.
6. Kaplan, Z., Saphier, D., Melnik, D., Gorelic, Z., Ashkenazy, J., Sudai, M., Kimhe, D., Melnik, M., Smith, S., and Juhasz, A., "Electrothermal Augmentation of a Solid Propellant Launcher," *IEEE Transactions on Magnetics* **29** (1), 1993, pp. 573-578.
7. Li, J. Q., Kwon, J., Thynell, S. T., and Litzinger, T. A., "Experimental investigations of characteristics of electro-thermal-chemical plasma," AIAA Paper 2001-3855, Joint Propulsion Conference, Salt Lake City, Utah, July 8-11, 2001.
8. Thynell, S. T., Zhou, H., Li, J. Q., and Litzinger, T. A., "Experimental study on the transient interaction between a plasma and a propellant," *Proceedings of the 36th JANNAF Combustion Subcommittee Meeting*, CPIA Publications 691, October 1999, pp. 119-132.
9. Ryan, M., Clemens, N. T., and Varghese, P. L., "Measurements In A Pulsed Electrothermal Plasma Jet," Paper 2004-0388, AIAA 42nd Aerospace Sciences Meeting, Reno, January 2004.
10. Ryan, M. D., Clemens, N.T. and Varghese, P.L., "Optical Measurements of the Interaction Between Electrothermal-Plasmas and Solid Propellants," Paper 4I-02, 40th JANNAF Combustion Subcommittee Meeting, Charleston, SC, June 2005.
11. Ryan, M., Clemens, N. T., and Varghese, P. L., "Spectroscopic Measurements During an Electrothermal Plasma-JA2 Solid Propellant Interaction," Paper 2006-1464, AIAA 44th Aerospace Sciences Meeting, Reno, January 2006.

## MEASUREMENTS OF ELECTROTHERMAL-PLASMA IGNITION OF SOLID PROPELLANTS

Michael D. Ryan<sup>\*</sup>, Noel T. Clemens<sup>†</sup> and Philip L. Varghese<sup>‡</sup>  
Center for Aeromechanics Research  
The University of Texas at Austin, Austin, Texas 78712-1085

### ABSTRACT

The work presented is part of continuing experimental study of the ignition of solid propellants by electrothermal capillary plasmas. Experiments have been made to characterize further the pulsed plasma expanding into room air and to investigate ignition of JA-2 propellant in a closed chamber. A particular emphasis is placed on discussing the difficulties in conducting diagnostics in this challenging environment. Heat flux measurements were made with a heat flux sensor along the axis of the plasma-jet. Measurements were made with and without a fused silica flat covering the sensor to enable the measurement of radiative and total heat flux, respectively. Radiative heat flux was found to be a substantial fraction of the total heat flux and the peak heating tended to occur well after the plasma luminosity had dissipated. Experiments employing planar laser-induced fluorescence (PLIF) of atomic copper showed that the very large background luminosity of the plasma greatly limits the quality of the measurements. The high luminosity has necessitated the use of two-cameras to enable single-shot background subtraction. Experiments in a closed chamber indicate that the propellant can be successfully ignited with the plasma, but it appears that the formation of fine particulates due to condensation of the plasma may significantly hinder the use of optical diagnostics.

### INTRODUCTION

Studies of propellant charges ignited by plasma discharges have shown that this technique has significant advantages over conventional (primer) ignition.<sup>1-8</sup> It has been shown that ignition delay and jitter were substantially reduced, and temperature compensation achieved, with a plasma energy input that was substantially smaller than the energy required to heat the propellant bed to the reference condition. However, the mechanism that is responsible for the improved performance is unknown. The plasma could function merely as an improved thermal source since it has a very high temperature compared to conventional combustion products. It could function as a radiant source that distributes the energy into the propellant bed more uniformly and rapidly than simple flame spread.

Additionally, the plasma could provide a source of highly reactive species, not present in flames, which promote rapid and reliable ignition. In some configurations, plasma jets issuing into the propellant beds may penetrate more effectively than combustion products from a primer, and thus give a more distributed ignition. It is also possible that the blast wave accompanying the plasma discharge causes microfractures in the propellant grains that increases the burning surface area sufficiently to provide temperature compensation, though it seems hard to reconcile the observed repeatability of the process with known mechanisms of microfracture.

A combination of several of these mechanisms might also contribute to the observed performance improvement. An improved fundamental understanding of the interaction will help the Army design better initiators that tailor the plasma to the propellant, and thus reducing energy required or enhancing gun performance. For example, it may be possible to achieve the observed temperature compensation with a much smaller energy input than is currently needed, which would reduce the size of the power source required. Furthermore, because of the current lack of understanding, one cannot rule out the possibility that the plasma is interacting with only a minor component of the propellant charge, and thus plasma igniters could fail because of minor changes in propellant composition.

Owing to the complexity of the physical processes involved in plasma-induced ignition, achieving an understanding of the fundamental physics will likely be achieved only through computational/theoretical approaches aided by experimental data. To date, however, there is insufficient experimental data on the plasma-propellant interaction to properly develop and validate chemical models. Therefore, the primary goal of this project is to aid in this effort by experimentally studying the interaction of an electrothermal capillary plasma with solid propellants. This involves both the characterization of the electrothermal plasma source itself, as well as the plasma-ignition of a solid propellant in a confined reactor.

---

<sup>\*</sup> Graduate Student, ASE-EM Dept.

<sup>†</sup> Associate Professor, ASE-EM Dept., Associate Fellow AIAA

<sup>‡</sup> Professor, ASE-EM Dept., Associate Fellow AIAA

Copyright © 2004 by M. D. Ryan, N. T. Clemens and P. L.

Varghese. Published by American Institute of Aeronautics and Astronautics, Inc. with permission.

The major objective of this work is to generate as complete a picture as possible of the plasma-propellant interaction and subsequent ignition. This is being accomplished by the application of a range of diagnostics including emission spectroscopy, heat flux sensors, high-framing rate visible luminosity imaging and planar laser-induced fluorescence (PLIF). The PLIF is directed at obtaining the spatial distributions of species that either mark the plasma (e.g. atomic copper), or provide important information about the state of combustion (e.g. OH and NO).

The plasma-propellant flow field is a very challenging environment in which to make measurements because of the high temperatures and densities, complex chemistry, transient nature of the interaction, and high electrical noise caused by the pulse forming network. This paper can be considered to be a progress report that describes some recent results and some of the problems that have been encountered while working in this difficult environment. We describe our efforts at characterizing the electrothermal capillary plasma with fast-response heat flux measurements and PLIF of atomic copper, as well as preliminary kilohertz imaging of the plasma-ignition of JA-2 propellant inside a combustion chamber.

## EXPERIMENTAL SET-UP

Many of the features of the experimental set-up have been described previously<sup>9-11</sup> and are briefly summarized here. The capillary plasma source is driven by a pulse forming network (PFN), consisting of a 251  $\mu\text{F}$  capacitor charged to a maximum of 5.0 kV (3.1 kJ) and a 26  $\mu\text{H}$  inductor. The discharge is initiated by closing an Ignitron switch that connects the capacitor to the capillary electrodes. The capillary is 3 mm in diameter by 30 mm long and is open at one end only. The wall material is polycarbonate (Lexan,  $\text{C}_{16}\text{H}_{14}\text{O}_3$ ). To help initiate the discharge a thin copper or aluminum fuse wire (64  $\mu\text{m}$ ) is inserted inside the capillary between the electrodes. The wire explodes when the Ignitron is closed. Ablation and ionization of material from the capillary surface then sustains the discharge. The resulting plasma expands rapidly from the open end of the capillary and issues into room air or a closed chamber. In either case a highly under-expanded jet with a characteristic barrel shock structure is seen for most of the plasma pulse (duration approximately 250  $\mu\text{s}$ ). The peak current through the plasma is approximately 4.6 kA for a discharge energy of 5 kV (3.1 kJ). In order to reduce erosion, the electrodes were constructed with inserts made of copper-tungsten alloy (30% Cu, 70% W). A schematic of the plasma jet firing assembly is shown in Fig. 1.

In experiments aimed at characterizing the pulsed plasma jet, the jet is allowed to issue vertically into room air, as shown schematically in Fig. 2. Heat flux

measurements were made along the axis of the freely-expanding plasma-jet. The measurements were made by using a heat flux sensor (Vatell) with a response time of 6  $\mu\text{s}$ . The sensor was mounted at the end of a rod, as shown in Fig. 3, and was positioned at several standoff distances ( $x_s$ ) from the capillary bore exit. Because the plasma firing is such a short event, purely radiative heat flux measurements were taken by placing a fused silica flat in front of the sensor. In addition, total heat flux was measured at different points along the axis of the jet. Firings were repeatable enough so that radiative heat flux could be subtracted from total heat flux to find the conductive and convective (cc) heat flux by itself.

PLIF imaging of atomic copper is being developed to provide a marker of the plasma when ignition takes place in the combustion chamber. As a first step toward this end Cu PLIF is being applied in the freely expanding plasma jet as well. For Cu PLIF we pump the  $^2\text{P}_{3/2} \leftarrow ^2\text{S}_{1/2}$  line at 327 nm and detect the fluorescence from the  $^2\text{P}_{3/2} \rightarrow ^2\text{D}_{5/2}$  line at 578 nm. As shown in Fig. 2, the laser source is a Nd:YAG-pumped dye laser tuned to 654 nm, which was then frequency doubled to 327 nm. The laser was operated at 10 Hz, with energy per pulse of about 10 mJ. The laser triggers a custom-designed electronic circuit, which provides for the synchronization of the laser and transient plasma. The fluorescence was imaged with either one or two intensified CCD cameras (Princeton Instruments) gated to about 30 ns to help reject the high background luminosity. The cameras were fitted with 50 mm focal length, f/1.4 camera lenses and interference filters (3 nm bandwidth) to help reject background luminosity. For the two-camera experiments one camera captured the fluorescence and the other was gated just after the fluorescence terminated to provide a background image so that single-shot background subtractions could be used. The reason for this is that the fluorescence signals are very low compared to the background luminosity and so single-shot background corrections can help to improve the signal-to-background ratio of the measurements.

Our experiments on plasma-propellant interactions to date have been performed on JA-2 propellant with a composition shown in Table 1. The propellant is supplied in flexible-sheet form with a thickness of 2.5 mm (nominally 0.1 in). Note that preliminary ignition experiments with the plasma issuing into room air and impinging normally on the propellant surface did not lead to ignition, and hence the closed combustion chamber shown in Fig. 4 was constructed to confine the plasma. Sample disks of diameter 12 mm were cut from this sheet and attached to a support rod mounted inside the combustion chamber. The plasma-jet issues normal to the propellant disk. The chamber includes three windows to provide optical access for the laser sheet and imaging. Furthermore, a measurement port has been machined to enable pressure measurements in the

chamber during the discharge by using a fast-response pressure transducer (Kistler, 10,000 psi).

Interactions of the plasma with the propellant sample led to propellant ignition for initial capacitor voltages of 3.6 kV or greater. The corresponding discharge energy is 1.6 kJ

### **PRELIMINARY RESULTS**

Figure 5 shows a representative image of the visible luminosity of the plasma jet issuing into room air. This image was obtained for an initial charging voltage of 3 kV (1.1 kJ) and was captured 95  $\mu$ s after the initiation of the discharge. The gate-width (exposure time) used was 85 ns which was sufficiently small to freeze the flow. The barrel shock, Mach disk, contact surface and luminous bore-exit flow are clearly seen in the emission image. Our previous studies using line-of-sight average emission spectroscopy suggest that the excitation temperatures in the plasma-jet range from about 15,000 within the barrel shock to about 25,000 K downstream of the Mach disk, and with electron number densities that are of order  $10^{17}$  to  $10^{18}$  cm<sup>-3</sup>.<sup>9,10</sup>

Figure 6 shows the radiative flux recorded by the heat-flux sensor along the axis of the plasma jet. The measurements were made as a function of sensor standoff distance. To obtain the radiative heat transfer the sensor was shielded by a fused-silica flat. Figure 7 shows the total flux measured with the silica flat removed. Significant electromagnetic interference was observed in the total flux measurements made closer to the capillary exit, as shown in the record made at  $x_s=47$  mm from the capillary. Figure 8 shows the values of the peak heat flux for each location along the axis of the jet for both radiative and conductive/convective flux cases. Also included on the figure is the time taken to reach the peak heat flux at that location. Electromagnetic interference from the plasma was too great to get a reliable peak heat flux for the conductive and convective case for  $x_s = 47$  and 72 mm.

Peak radiative and cc heat flux both decrease along the jet axis, which is to be expected. Also, the time to peak heating increases with axial distance with the exception of peak radiative flux at a distance of 174 mm. Peak conductive and convective flux is greater than radiative flux at the axial distances tested, but they are of the same order of magnitude. It is interesting to note that peak flux times for both cases generally occur at times that are well after the intense visible luminosity has diminished. Although conductive and convective heat fluxes would be expected to occur later in the discharge, the observed time of peak heat flux is much later than the time required for the hot plasma to move down stream. The heat flux due to conduction from the metal housing surrounding the sensor is expected to be much smaller ( $<500$  W/cm<sup>2</sup>). This was estimated from the maximum increase in sensor temperature ( $\sim 30$  K).

One possible explanation of these observations is that the sensor detects radiation from the hot electrode. This radiation is absorbed by the plasma during the discharge, but after the discharge dissipates the heat flux sensor “sees” the electrode. To test this hypothesis the sensor was placed at an angle so that it was not in the line-of-sight of the bore exit. The resulting heat flux time history is shown in Fig. 6 with the label “angled,” and it shows that indeed the heat flux is significantly lower when out of the line of sight of the bore.

Figure 9 shows two representative Cu PLIF images obtained in the plasma-jet issuing into room air. Figure 9a is an image captured when using an aluminum fuse wire to initiate the plasma, whereas Fig. 9b shows an image using a copper fuse wire. These single-camera images include both the fluorescence and the background luminosity. Arrows in each figure show the location of the laser sheet and careful inspection reveals a weak fluorescence signal above the background. These images show the difficulty of doing PLIF in such a luminous flow. Despite the fact that we have a very large degree of background rejection, owing to the combined 30 ns gate and line filter, the signal-to-background ratio is still very low. From the signal shot noise in regions outside of the luminous regions, it appears that the signals are relatively high. This suggests that the problem is due to high background rather than low signal. The high background is the reason for using single-shot background subtraction.

Also, an interesting feature of Fig. 9b is that it seems that the laser sheet is strongly absorbed at the left edge of the plasma jet, when a copper fuse wire is used. This same absorption does not occur with the aluminum fuse-wire, and so this suggests that atomic copper from the exploded copper fuse wire absorbs much of the laser power on the outer edges of the plasma before laser light hits the barrel shock. This is undesirable so we now use only aluminum for the fuse wire.

Figure 10 shows an average, background-corrected PLIF image of Cu in the pulsed plasma jet, which was taken in a previous study in our laboratory.<sup>11</sup> The image represents a 17 shot average that was corrected by subtracting a 17 shot average background image. Figure 10 shows that Cu PLIF reveals a very different structure of the flow as compared to the natural luminosity. In fact, the PLIF image shows that the luminous plasma jet is surrounded by a shroud of atomic copper that is not luminous and so is presumably cold. We believe that the shroud of cold copper comes from the exploding wire used to initiate the discharge, whereas the smaller copper signal in the barrel shock comes from copper eroding from the Cu-W electrode during the discharge.

The two-camera PLIF technique is still in a preliminary stage. The two cameras view the same field

of view in the plasma by using a beam-splitting cube. One camera captures the fluorescence and background with a 30 ns gate, and the other captures the background 5 ns after the end of the first camera's gate. The resolution of each camera was quantified by measuring the line-spread function. It was found that the cameras have the same line-spread function and hence the same frequency response to within the measurement uncertainty. Furthermore, in order to accomplish a background subtraction, the cameras must be registered to sub-pixel accuracy. To do this one must take into account not only the global field of view differences (translation, rotation, magnification, angular distortion), but also intrinsic distortion effects of each camera system. By taking an image of a grid (dot card) with both cameras, the cameras were geometrically transformed (or warped) onto a regular grid. A Matlab code was written that performed this transformation and subsequent bilinear interpolation to match up each camera image pixel by pixel.

Once the camera images could be suitably registered, a study was conducted to determine the optimum gain settings for each camera. While the field of view might be matched through image processing, if the relative intensifier response is not a constant or some known function of intensity, then it is impossible to accurately subtract the background emission. The lowest f-stop was chosen to keep the signal-to-noise ratio as high as possible even though there is some cost in resolution. Low intensifier gains were selected so that the relative intensity response was essentially linear over the range of intensities seen in the plasma. This minimizes problems due to noise and the nonlinear responses of the intensifiers.

The accuracy of a single shot background subtraction is shown in Fig. 11. Images of the plasma were taken by both cameras by using the same timing as that of the PLIF experiment. An average image of the plasma emission from each camera was computed and then the ratio of these average images was computed. A single shot plasma image from one camera was multiplied by the ratio-image to emulate the second camera image of the same firing. If the correction is perfect, when the emulated and other camera images are subtracted, the result will be a null image. Figure 11 shows the correction procedure is not perfect as the percent variation between the second camera image and the emulation is about  $\pm 20\%$  outside of the jet exit. These relatively high residual variations are likely due to registering errors, non-uniform responsivity of the intensifiers and nonlinear response of the intensifiers. It is clear that it will probably not be possible to obtain true single-shot background corrected images because the fluorescence signal is less than 20% of the maximum of the background. Nevertheless, good mean PLIF images should be possible because the

variations are random and so they should average to zero

Figure 12 shows a sequence of images of the visible luminosity for the case of plasma-ignition of JA-2 in the combustion chamber. The initial discharge voltage and energy were 4 kV and 2 kJ, respectively. These images were taken with a Kodak Ektapro HS4540 at a framing rate of 13,500 frames per second. The distance between the exit of the plasma jet and the JA-2 disk was about 20 mm. The sequence is actually a composite assembled from different runs, because a single camera/lens setting does not have sufficient dynamic range to capture the range of intensities that occur over the duration of a run. In these images the plasma axis is horizontal and it travels left to right. The propellant disk (12 mm diameter) is vertical and is labeled in the second image.

The first image, captured at 0.222 *ms* from the start of the plasma discharge, shows the structure of the impinging plasma jet. The luminous bore exit can be seen at left and the very luminous Mach disk is seen as the triangular shaped region at right. At this instant the propellant is enveloped in the plasma. At 1.48 *ms* the high plasma luminosity has largely dissipated, although swirling lower-luminosity gas can still be seen in the videos. It should also be noted that the side of the propellant mounting rod can be seen in the image. Interestingly, at 10 *ms* the rod is no longer visible. At between 30-50 *ms* the videos show bright luminous specks are ejected from the surface of the propellant, which presumably marks the beginning of ignition. Such specks can be seen at 50, 100 and 150 *ms* in Fig. 12.

We attempted to make PLIF measurements on OH in the closed chamber to study the ignition of the propellant after interaction with the plasma. However, no PLIF signal could be detected. In an attempt to diagnose the problems associated with the experiment we transmitted a He-Ne laser beam across the chamber and imaged the laser spot produced on a card with the high speed camera. We observed that the spot disappeared a few milliseconds after the plasma pulse and did not return for hundreds of milliseconds later. The extinction occurred both with and without propellant in the chamber. The similar effect can be seen in Fig. 12 when the surface of the rod is no longer visible. We believe that the extinction is due to scattering by nano-particles that are formed by the cooling plasma. This is potentially a major problem for the use of laser diagnostics in the closed-chamber and this effect is currently under investigation.

## **SUMMARY AND FUTURE WORK**

The work presented is part of continuing experimental study of the ignition of solid propellants by electrothermal capillary plasmas. Experiments have

been made to characterize further the pulsed plasma jet expanding into room air and to investigate ignition of JA-2 propellant in a closed chamber. Heat flux measurements were made with a fast-response heat flux sensor for varying positions along the axis of the plasma-jet. Measurements were made with and without a fused silica flat covering the sensor to enable the measurement of radiative and total heat flux, respectively. Radiative heat flux was found to be a substantial fraction of the total heat flux and the peak heating tended to occur well after the plasma luminosity had dissipated. The latter observation is likely because the sensor detects the “glow” from hot capillary bore once the plasma dissipates. Experiments employing PLIF of atomic copper showed that the very large background luminosity of the plasma greatly limits the quality of the measurements. Nevertheless, high quality mean images of Cu could be acquired and these show that a “shroud” of cold, low-luminosity copper surrounds the luminous plasma jet. To improve upon these results, we are developing a two-camera technique that will enable single-shot background subtraction. Experiments in a closed chamber indicate that the propellant can be successfully ignited with the plasma, but it appears that the formation of fine particulates due to condensation of the plasma may significantly hinder the use of optical diagnostics. This latter point is an important finding and will be aggressively investigated in future work.

### **ACKNOWLEDGEMENTS**

This work was supported by the Army Research Office under Grant No. DAAD19-00-1-0420. The grant monitor is Dr. David Mann. The Cu PLIF measurements described in Ref. 11 were made at UT Austin by Dr. J.U. Kim while he was a post-doctoral fellow working with Profs. Clemens and Varghese.

### **REFERENCES**

1. Shaw, R.W., Mann, D.M., Anderson, W.R., White, K., Nusca, M.J. and Powell, J., “Army Plasma/Propellant Interaction Workshop – U.S. Army Research Office 17-18 November 1998,” Report No. ARL-SR-83, November 1999.
2. Oberle, W., White, K. and Powell, J., “JANNAF Combustion Subcommittee Workshop: Plasma / Propellant Interaction and Propellant Temperature Sensitivity Reduction Using Electrothermal-Chemical (ETC) Propulsion Concepts.” Report ARL-TR-1579, U.S. Army Research Laboratory, Aberdeen Proving Ground, MD, December 1997.
3. Edwards, C., Bourham, M. and Gilligan, J., “Experimental studies of the plasma-propellant interface for electrothermal-chemical launchers,” *IEEE Transactions on Magnetics* **31** (1), p. 404-409, 1995.
4. Greig, J. R., Earnhart, J. R., Winsor, N., McElroy, H. A., Juhasz, A. A., Wren, G. P., and Morrison, W. F., “Investigation of Plasma Augmented Solid Propellant Interior Ballistic Processes,” *IEEE Transactions on Magnetics* **29** (1), 1993, pp. 555-560.
5. Woodley, C. R., “A Parametric Study for an Electrothermal-Chemical Artillery Weapon,” *IEEE Transactions on Magnetics* **29** (1), 1993, pp. 625-630.
6. Kaplan, Z., Saphier, D., Melnik, D., Gorelic, Z., Ashkenazy, J., Sudai, M., Kimhe, D., Melnik, M., Smith, S., and Juhasz, A., “Electrothermal Augmentation of a Solid Propellant Launcher,” *IEEE Transactions on Magnetics* **29** (1), 1993, pp. 573-578.
7. Li, J. Q., Kwon, J., Thynell, S. T., and Litzinger, T. A., “Experimental investigations of characteristics of electro-thermal-chemical plasma,” AIAA paper 2001-3855, Joint Propulsion Conference, Salt Lake City, Utah, July 8-11, 2001.
8. Thynell, S. T., Zhou, H., Li, J. Q., and Litzinger, T. A., “Experimental study on the transient interaction between a plasma and a propellant,: Proceedings of the 36th JANNAF Combustion Subcommittee Meeting, CPIA Publications 691, October 1999, pp. 119-132.
9. Kohel, J. M., Su, L. K., Clemens, N. T. and Varghese, P. L., “Emission Spectroscopic Measurements and Analysis of a Pulsed Plasma Jet,” *IEEE Transactions on Magnetics* **35** (1), 1999, pp. 201-206.
10. Kim, J. U., Clemens, N.T. and Varghese, P.L., “Experimental Study of the Transient Underexpanded Jet Generated by an Electrothermal Capillary Plasma,” *AIAA J. Propulsion and Power* **18** (6), 2002, pp. 1153-1160.
11. Kim, J. U., Clemens, N.T. and Varghese, P.L., “Characterization of a High-Density Plasma Produced by Electrothermal Capillary Discharge,” *Applied Physics Letters* **80**, pp. 368-370, 2002 and **80**, p. 2806, 2002 (Erratum).

Table 1 Composition of JA-2 Propellant

Constituent	% by mass
Nitrocellulose	58.14
Nitroglycerine	15.82
Diethylene glycol dinitrate	25.23
Akardit II	0.71
Magnesium oxide	0.05
Graphite	0.05
Total	100.0

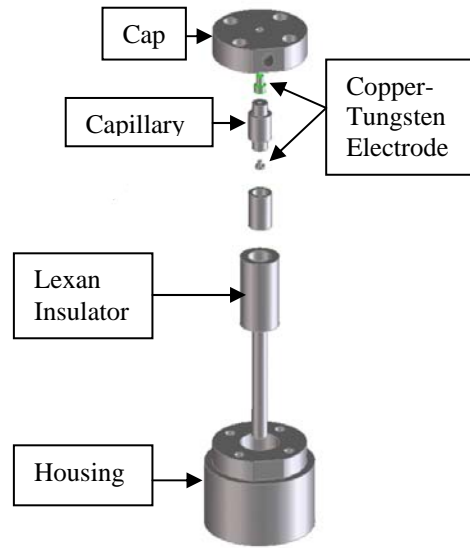


Figure 1. Schematic of plasma jet firing assembly.

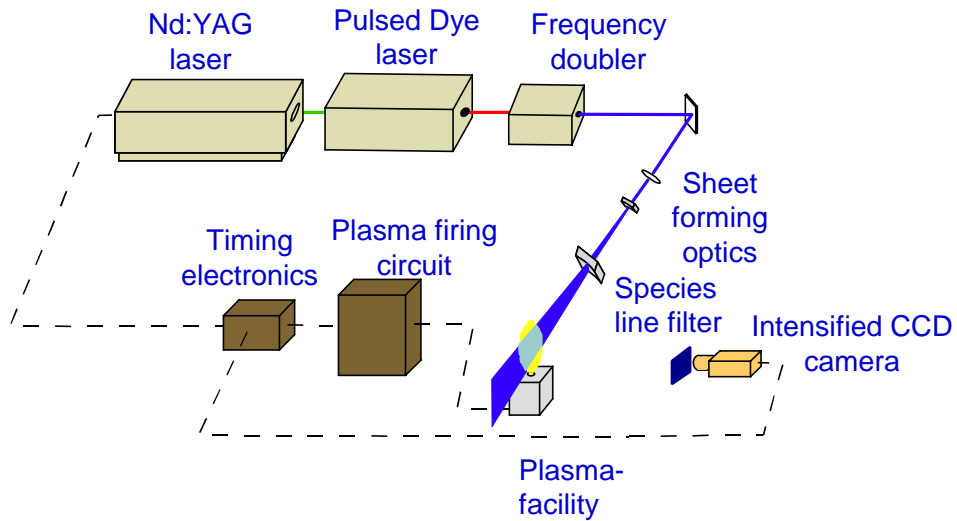


Figure 2. Experimental set-up for the PLIF imaging of the plasma-jet.

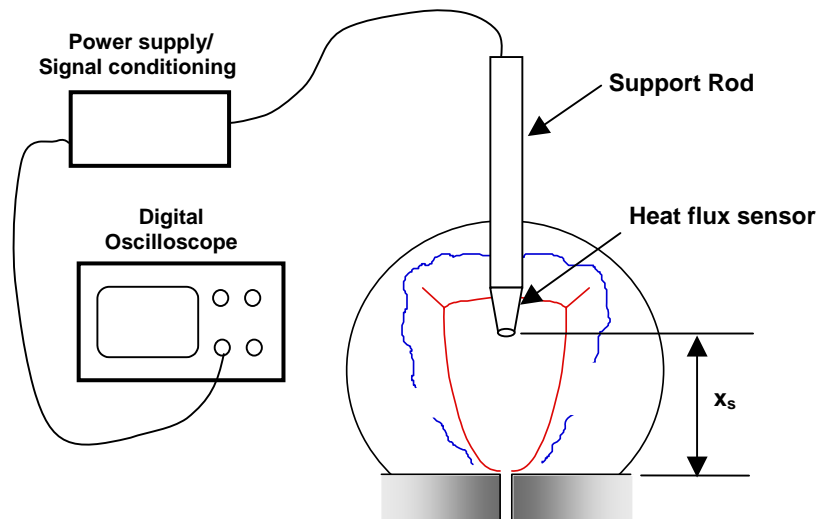


Figure 3. Experimental setup for heat flux measurements. The sensor standoff distance is  $x_s$ .

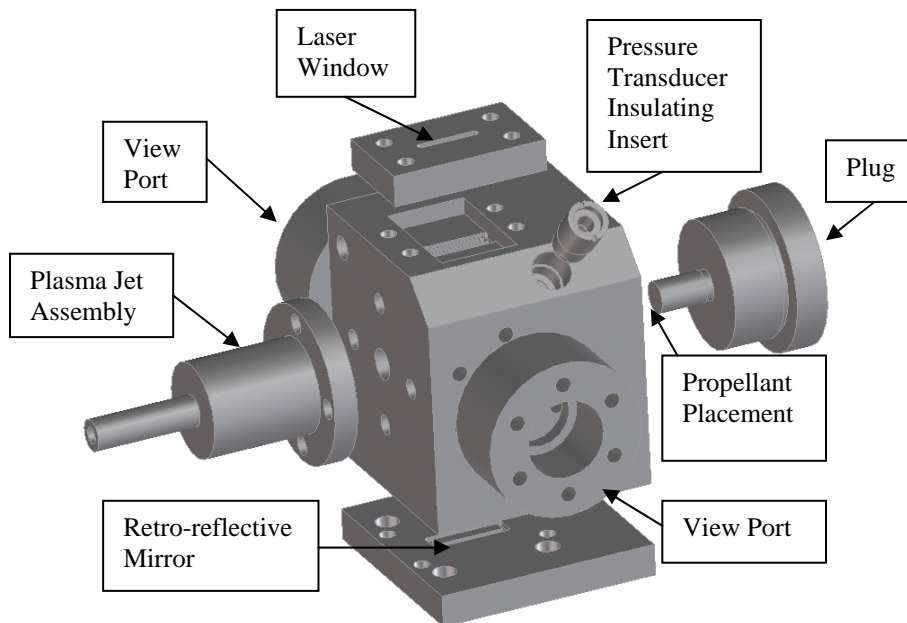


Figure 4. Closed combustion chamber with windows for viewing and laser passage

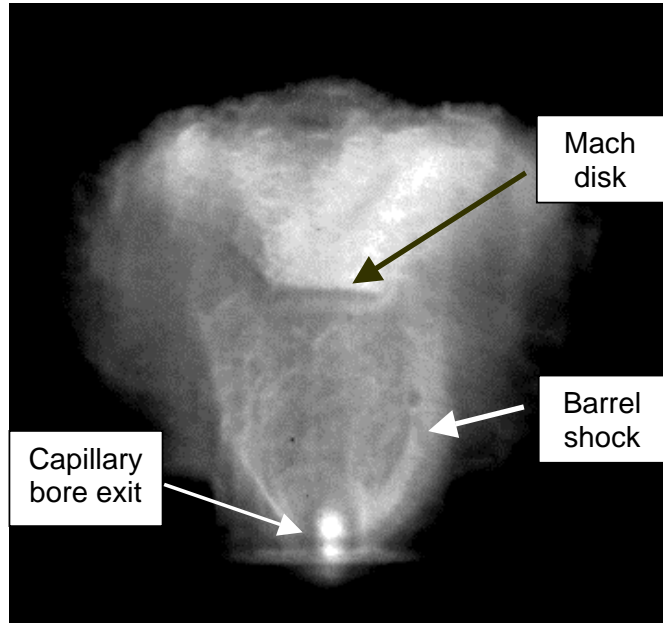


Figure 5. ICCD Image of the visible luminosity of the plasma jet issuing into room air. The camera was gated to 85 ns and the image was taken with a delay of 95  $\mu$ s from the initiation of the discharge.

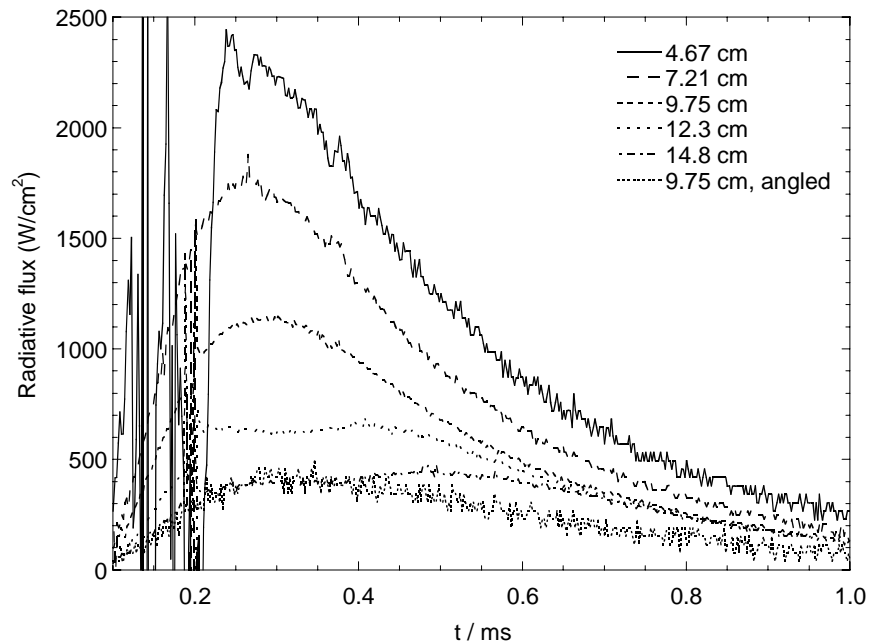


Figure 6. Time-dependent radiative heat flux measurements at several axial locations.

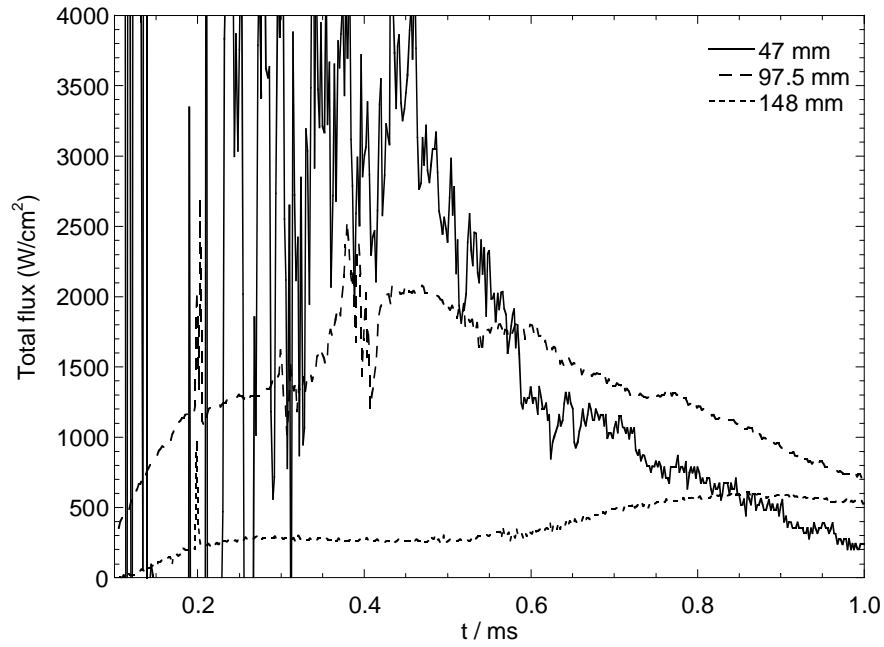


Figure 7. Time-dependent total heat flux measurements at several axial locations.

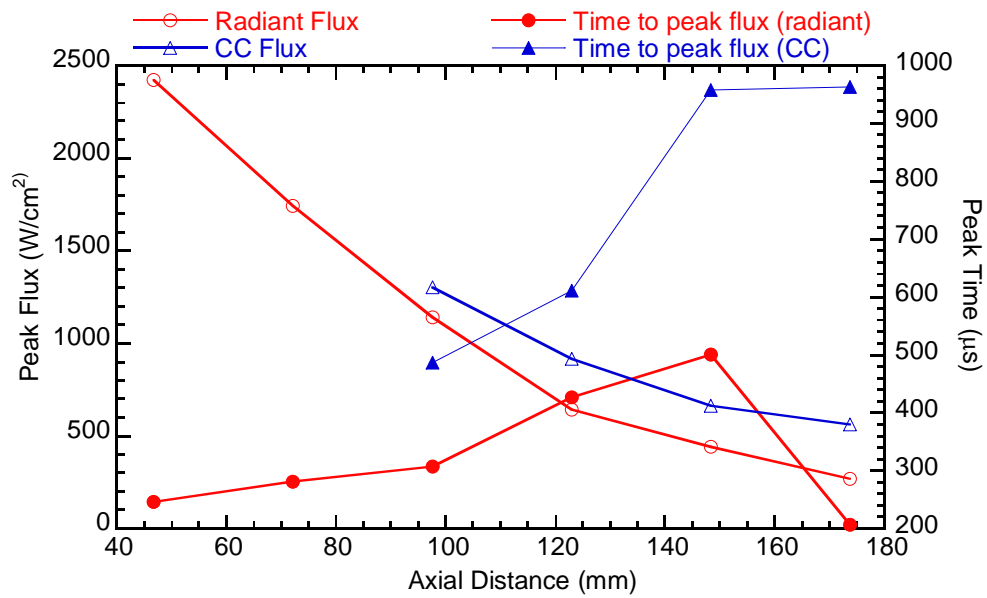


Figure 8. Variation of heat fluxes and time of the peak heat flux after discharge initiation with downstream location.

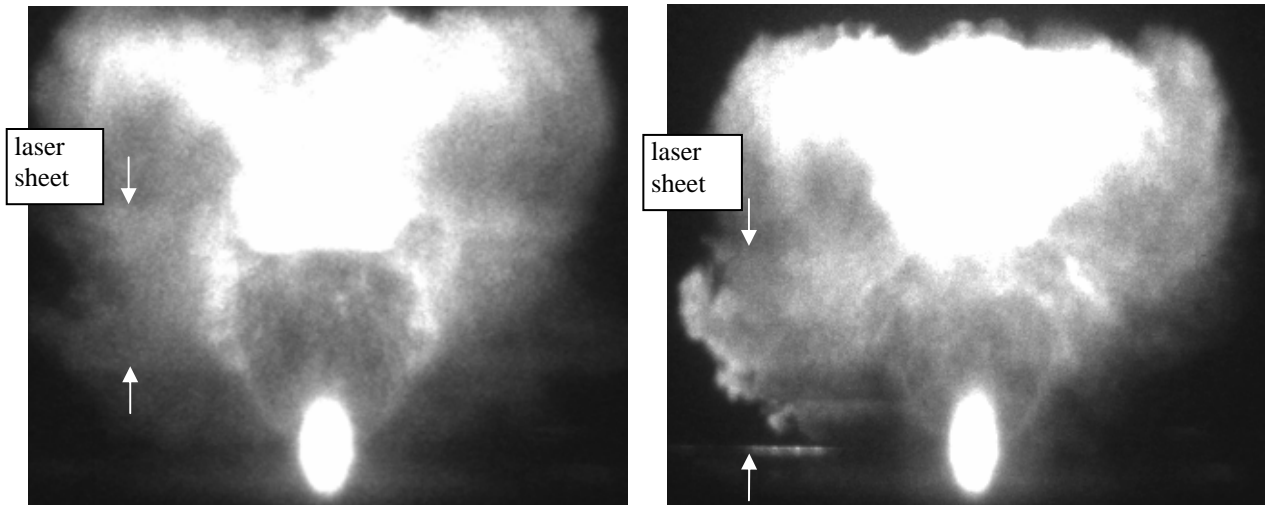


Figure 9. Single-shot Cu PLIF images. (a) aluminum fuse wire, (b) copper fuse wire.

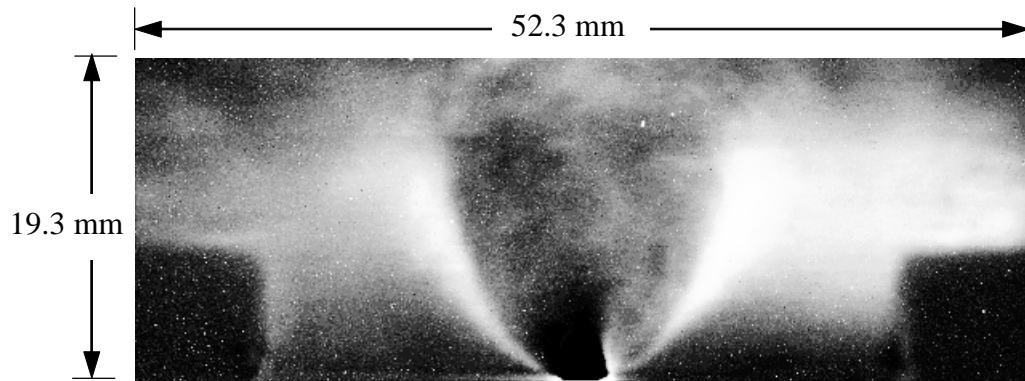


Figure 10. Grey scale image of Cu atoms detected by PLIF. 17 PLIF images were averaged, and background subtracted using a 17 shot average of plasma emission only. The excitation laser beam is passing from left to right and is retroreflected. (From Kim et al., 2002).

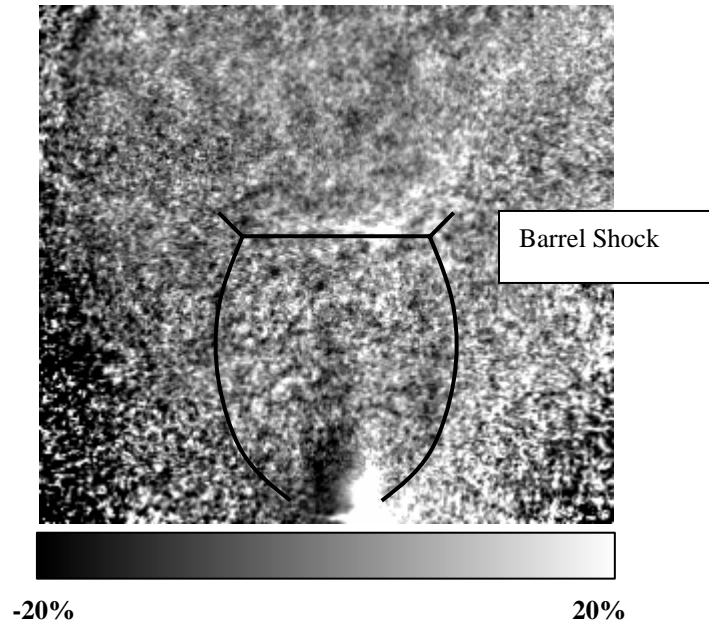


Figure 11. Percent variation of residual after background subtraction.

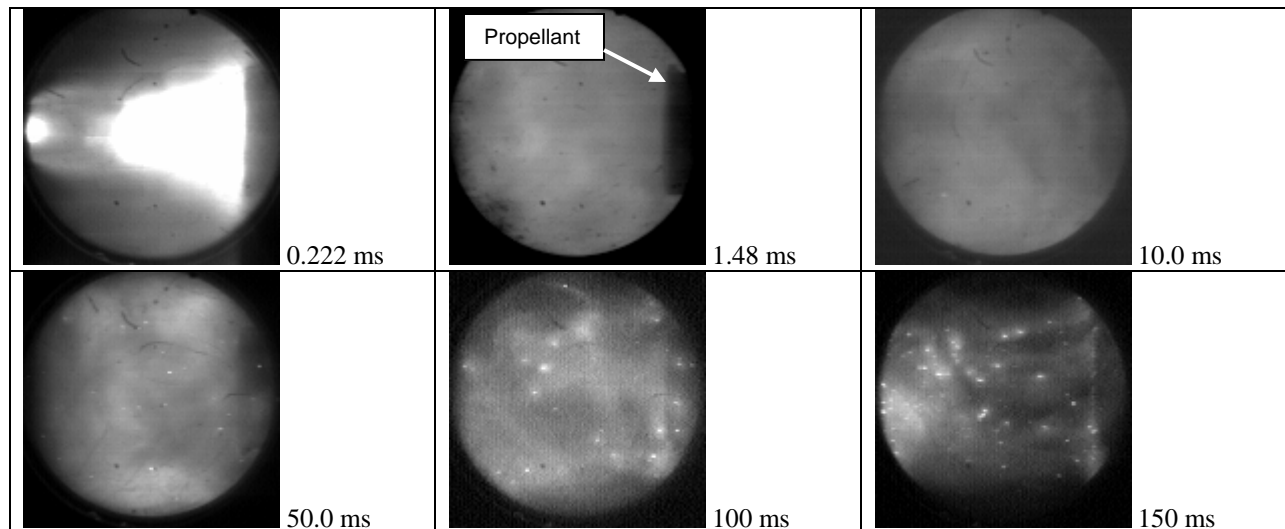


Figure 12. Visible-luminosity images of plasma-ignition of JA-2. The images were acquired at a framing rate of 13,500 frames per second.

**OPTICAL MEASUREMENTS OF THE INTERACTION BETWEEN ELECTROTHERMAL-PLASMAS  
AND SOLID PROPELLANTS**

Michael D. Ryan, Noel T. Clemens, and Philip L. Varghese

Center for Aeromechanics Research

The University of Texas at Austin

Austin, Texas

**ABSTRACT**

The work is part of continuing experimental study of the ignition of solid propellants by electrothermal capillary plasmas. Experiments have been conducted to characterize the pulsed plasma expanding into room air and to investigate ignition of JA-2 propellant in a closed chamber. The plasma emerges from the capillary as a highly-underexpanded transient jet. Gated emission spectroscopy was used to estimate the plasma temperature along the centerline of the plasma jet near the surface of a propellant disk. The experimental difficulties in making measurements in this challenging environment are discussed. Experiments in a closed chamber indicate that the plasma has sufficient energy to ignite the propellant successfully. However, the formation of fine particulates due to condensation of the plasma significantly hinders the use of optical diagnostics. Open-air experiments provide good optical access to study the plasma-propellant interaction. The propellant begins to decompose when exposed to the plasma directly or when exposed to plasma radiation alone, though the lack of confinement prevents ignition. Experiments employing planar laser-induced fluorescence (PLIF) showed that the very large background luminosity of the plasma, and laser light scattering from condensing microparticles limits the quality of the measurements.

**INTRODUCTION**

Electrothermal plasma ignition of solid propellants in tank guns has been studied with the hope that plasma ignition would improve gun performance over conventional primer ignition. An electrothermal plasma, formed from the discharge of high voltage capacitors through a plastic capillary, usually ignites propellant by jetting out one end of the capillary into the propellant. It was thought that the higher energy of the plasma igniter over a conventional igniter might increase the burning rate of the propellant and augment the pressure in the bore resulting in increased muzzle velocity. Early studies did find increased muzzle velocities,<sup>1,2</sup> although the ~5% increase was lower than expected. However, these and other<sup>3,4</sup> tests discovered additional benefits from plasma ignition in the form of reduced ignition delay and jitter<sup>3</sup> as well as temperature compensation of the propellant.<sup>4</sup> While plasma ignition of solid propellants showed pressure augmentation during propellant ignition,<sup>5</sup> the body of evidence seems to show that propellant burning rate (calculated from pressure data) is increased only in certain plasma propellant interaction geometries<sup>6</sup> and not in conventional gun designs substituting an electrothermal plasma for burning primer.<sup>7</sup>

Beyond pressure time histories inside a closed chamber, heat flux measurements, and time integrated atomic transition temperature measurements, very little work has been done to study the reacting fluid during the plasma propellant interaction (PPI). While knowledge of temporally resolved quantities like temperature and species concentrations during the interaction will not answer larger questions of gun performance, it could help modelers who do not presently have a detailed knowledge of the physical and chemical processes occurring during the PPI. This information would also benefit propellant designers who might tailor propellants to optimize pressurization and heat release effects during the PPI.

Optical diagnostic techniques are potentially invaluable for making temporally and spatially resolved measurements in a harsh environment such as the PPI because no physical probes need be introduced into the interaction region. While it would be desirable to conduct diagnostics inside a closed chamber as the propellant ignites, it has been found that condensates formed during plasma cooling severely attenuate lasers propagating through the fluid. Even at atmospheric pressure with plasma

impinging normally onto the propellant surface, where propellant reacts but does not ignite, particulates can complicate laser diagnostics. However, emission spectroscopy is possible in this environment and has been used to make temperature and electron density measurements. Because electrode ablation introduces atomic copper in to the plasma, it is possible to measure a plasma temperature from relative intensities of its emission lines of and assuming local thermodynamic equilibrium (LTE). This method has been used in the past at our lab to measure temperature in a plasma jet.<sup>8</sup> We have extended this work to include the temperature at the surface of propellant during a plasma propellant interaction.

By separating propellant from the electrothermal plasma with a window, it is possible to produce a reaction on the propellant surface resulting only from the plasma radiation. Recent studies of the PPI have focused solely on this aspect of the interaction.<sup>9</sup> There is evidence that radiation, because of its in-depth effect on translucent and transparent propellants (JA2 can be both), is the cause of increased burning rate in propellants after the PPI.<sup>10</sup> In a pure radiation interaction, problems with laser diagnostics inside the electrothermal plasma are obviated. We have begun work on time resolved planar laser induced fluorescence (PLIF) measurements of NO<sub>2</sub> and NO during the radiation interaction. Both species have been detected in thermal decomposition studies of nitrate ester propellants like JA2.<sup>11</sup>

The major objective of this work is to generate as complete a picture as possible of the plasma-propellant interaction and subsequent ignition. This is being accomplished by the application of a range of diagnostics including emission spectroscopy, heat flux sensors, high-framing rate visible luminosity imaging and planar laser-induced fluorescence (PLIF). The PLIF is directed at obtaining the spatial distributions of species that either mark the plasma (e.g. atomic copper), or provide important information about the propellant decomposition during ignition (e.g. NO and NO<sub>2</sub>).

The plasma-propellant flow field is a very challenging environment in which to make measurements because of the high temperatures and densities, complex chemistry, transient nature of the interaction, and high electrical noise caused by the pulse forming network. This paper is a progress report that describes some recent results and some of the problems that have been encountered while working in this difficult environment. We describe our efforts at characterizing the electrothermal capillary plasma with emission thermometry, kilohertz imaging of the plasma-ignition of JA-2 propellant inside a combustion chamber, and preliminary PLIF measurements of atomic copper and molecular species.

## EXPERIMENTAL SET-UP

Many of the features of the experimental set-up have been described previously<sup>8,12</sup> and are briefly summarized here. The capillary plasma source is driven by a pulse forming network (PFN), consisting of a 251  $\mu$ F capacitor charged to a maximum of 5.0 kV and a 26  $\mu$ H inductor. The discharge is initiated by closing an Ignitron switch that connects the capacitor to the capillary electrodes. The capillary is 3 mm in diameter by 30 mm long and is open at one end only. The wall material is polycarbonate (Lexan, C<sub>16</sub>H<sub>14</sub>O<sub>3</sub>). To help initiate the discharge a thin copper fuse wire (64  $\mu$ m) is inserted inside the capillary between the electrodes. The wire explodes when the Ignitron is closed. Ablation and ionization of material from the capillary surface then sustains the discharge. The resulting plasma expands rapidly from the open end of the capillary and issues into room air or a closed chamber. In either case a highly under-expanded jet with a characteristic barrel shock structure is seen for most of the plasma pulse (duration approximately 250  $\mu$ s). The peak current through the plasma is approximately 4.6 kA for a discharge energy of 5 kV (3.1 kJ). In order to reduce erosion, the electrodes were constructed with inserts made of copper-tungsten alloy (30% Cu, 70% W). A schematic diagram of the plasma jet firing assembly is shown in Fig. 1.

All timing is run off a 10 Hz signal from a pulse generator. Electronics, built in-house, are used to synchronize the firing of the plasma with the pulse generator when a button is pushed. Appropriate delays are produced by delay generators. The laser is also synchronized with the pulse generator using the delay generators. This allows the laser to run at 10 Hz (to keep it maximum pulse energy), while the firing and any camera triggering will be accurate to within 5 ns. Accurate timing is very important because of the large background plasma luminosity.

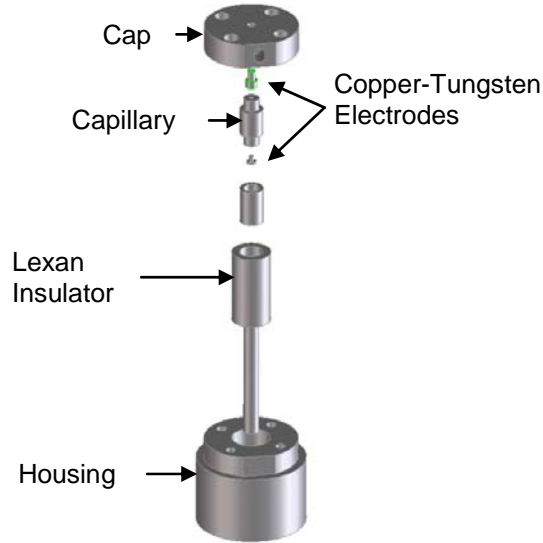


**Figure 1. Schematic diagram of plasma jet firing assembly.**

For the copper line temperature measurements the plasma jets into room air through the 3 mm cathode-nozzle. A 12 mm diameter disk of JA2 sheet propellant is placed 12 mm above the jet exit on the end of a steel rod so that the jet impinges normally to the surface. A lens focuses plasma light onto a fiber optic which a Spex 1681 spectrograph spectrally resolves and a Princeton Instruments PI-Max intensified CCD camera records. The spectrometer, gated to 1  $\mu$ s, records line of sight emissions spectra focused on the 3 mm closest to the propellant surface. Because image acquisition speed is much slower than 500  $\mu$ s, only one spectrum is taken per firing. However, firings are repeatable so that it is possible to measure a full time history of the temperature of the fluid at the propellant surface during the plasma discharge.

The spectrometer is set to record spectral data between 480-600 nm. The spectra are processed to account for differential wavelength response by the detector and differential response with respect to pixel number due to the spectrograph. Six copper emission peaks in this wavelength range, shown in Table 1, are then fit to Lorentzian lineshapes while simultaneously fitting surrounding lines and the background continuum luminosity (estimated as linear). The areas under each fitted emission lineshape are interpreted as total emission signal and are then compared on a Boltzmann plot. The points should fall on a line with the formula

$$\ln \left( \frac{I\lambda}{A_{ul}g_u} \right) = B - \frac{E_u}{kT_{exc}}.$$

Here  $I$  is the relative intensity of an emission line,  $\lambda$  is the emission wavelength,  $A_{ul}$  is the spontaneous emission rate, and  $g_u$  is the degeneracy or statistical weight factor for the excited (upper) state,  $B$  is a constant,  $E_u$  is the energy of the upper state,  $k$  is Boltzmann's constant, and  $T_{exc}$  is the excitation temperature. If the gas is in local thermal equilibrium  $T_{exc} = T$ , where  $T$  is the gas temperature. In practice the temperature is inferred from the slope of a straight line fit to the data.

Preliminary PLIF measurements with the plasma jet impinging directly on the propellant were plagued with interference problems, as described further below. Hence, we have begun a series of experiments where the plasma discharges into a 5 cm<sup>3</sup> chamber placed on top of the original jet exit. This confines the plasma and only permits radiative transfer to the propellant through a 12 mm diameter fused silica window that separates the plasma from the propellant. The chamber has a side vent 3 mm in diameter to prevent excessive metal deposition inside the chamber, and to prevent high pressures in the

chamber. The same propellant disks used in the temperature measurements are used in these experiments and the propellant surface is 25 mm from the inside surface of the window.

**Table 1. Copper emission lines used in temperature measurements**

Line #	$\lambda$ nm	$g_u$	$E_u$ eV	$g_l$	$E_l$ eV	$A_{ul}$ $\times 10^8 \text{ s}^{-1}$
1	510.55	4	3.816	6	1.389	0.020
2	515.32	4	6.190	2	3.785	0.60
3	521.82	6	6.191	4	3.816	0.75
4	529.25	8	7.735	8	5.394	0.109
5	570.02	4	3.816	4	1.642	0.0024
6	578.21	2	3.785	4	1.642	0.0165

The NO<sub>2</sub> fluorescence experiments were conducted with a Spectra Physics GCR-150 Nd:YAG laser frequency doubled to 532 nm. The laser is focused into a sheet normal to the surface of the propellant by a 255 mm focal length cylindrical lens then cut to a width of 6.3 mm by an aperture. NO<sub>2</sub> has a broadband visible absorption spectrum with four electronic states directly or indirectly interacting along with a complicated vibrational and rotational band structure.<sup>13</sup> The associated broadband fluorescence is imaged with a PI-Max intensified CCD camera while laser scattering is filtered with a 532 nm cut filter.

For NO fluorescence, a frequency doubled Nd:YAG is used to pump a Lumonics HyperDYE-300 dye laser. The output beam from the dye laser (~574 nm) is frequency doubled using a KDP crystal inside an Inrad Autotracker. The doubled dye beam is then combined with the residual IR beam from the YAG, which was separated from the 532 nm beam and time delayed to overlap the doubled dye beam. These two beams' polarizations are matched and then they pass through an Inrad KDP mixing crystal. The output beam is ~225 nm and used to pump the ground state NO at the surface of the propellant to the first excited electronic state,  $A^2\Sigma^+(v'=0) \leftarrow X^2\Pi(v''=0)$ . The fluorescence signal from the same electronic transition is detected with a PI-Max intensified CCD camera with a UG-5 filter used to attenuate laser scattering signal.

Our experiments on plasma-propellant interactions to date have been performed on JA-2 propellant with a composition shown in Table 2. The propellant is supplied in flexible-sheet form with a thickness of 2.5 mm (nominally 0.1 in). Sample disks of diameter 12 mm were cut from this sheet and attached to a support rod mounted inside the combustion chamber. The plasma-jet issues normal to the propellant disk. Interactions of the plasma with the propellant sample led to propellant ignition in a closed chamber for initial capacitor voltages of 3.6 kV or greater. The corresponding discharge energy is 1.6 kJ.

**Table 2 Composition of JA-2 Propellant**

Constituent	% by mass
Nitrocellulose	58.14
Nitroglycerine	15.82
Diethylene glycol dinitrate	25.23
Akardit II	0.71
Magnesium oxide	0.05
Graphite	0.05
Total	100.0

## RESULTS AND DISCUSSION

Figure 2 shows a representative image of the visible luminosity of the plasma jet issuing into room air. This image was obtained for an initial charging voltage of 3 kV (1.1 kJ) and was captured 95  $\mu$ s after the initiation of the discharge. The gate-width (exposure time) used was 85 ns which was sufficiently small to freeze the flow. The barrel shock, Mach disk, contact surface and luminous bore-exit flow are clearly seen in the emission image. Our previous studies using line-of-sight average emission spectroscopy suggest that the excitation temperatures in the plasma-jet range from about 15,000 K within the barrel shock to about 25,000 K downstream of the Mach disk, and with electron number densities that are of order  $10^{17}$  to  $10^{18}$   $\text{cm}^{-3}$ .<sup>8,12</sup>

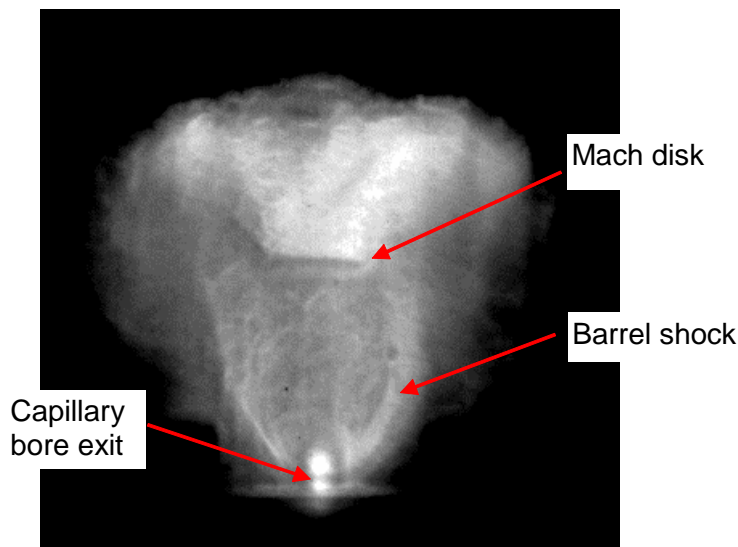


Figure 2. ICCD Image of the visible luminosity of the plasma jet issuing into room air. The camera was gated to 85 ns and the image was taken with a delay of 95  $\mu$ s from the initiation of the discharge.

Figure 3 shows the geometry used for the plasma jet impinging on a propellant disk. It also illustrates the difficulty of making PLIF measurements as discussed below. A laser light sheet at 532 nm to excite NO<sub>2</sub> fluorescence passes between the jet exit and the rod mounted propellant disk.

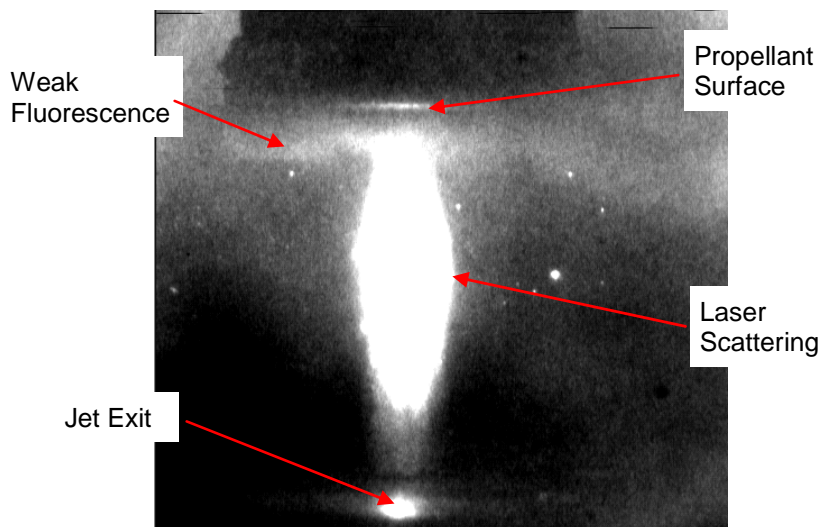


Figure 3. Open air plasma propellant interaction; NO<sub>2</sub> PLIF gray-scale image at 700  $\mu$ s delay.

A sample emission spectrum from the plasma impinging on a propellant disk is shown in Figure 4. The emission spectrum shown was collected 3 mm above the propellant surface at a delay of 60  $\mu$ s after discharge initiation. The spectral fit to obtain the relative intensity of the copper emission lines is also shown. The spectral fit includes the contributions of 7 separate lines, and includes Cu lines 1-4 from Table 1. Emission spectra were also collected near 570 nm to record the intensities of lines 5 and 6 of Table 1. A Boltzmann plot of the relative intensities is shown in Fig. 5.

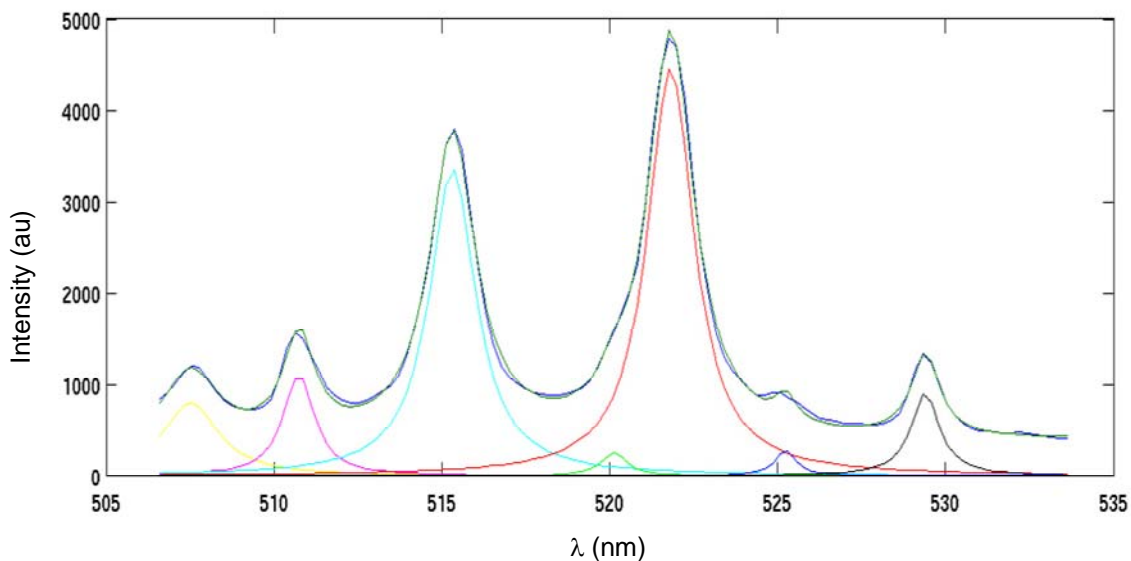


Figure 4. Plasma emission spectrum collected 3 mm from propellant surface at 60  $\mu$ s delay

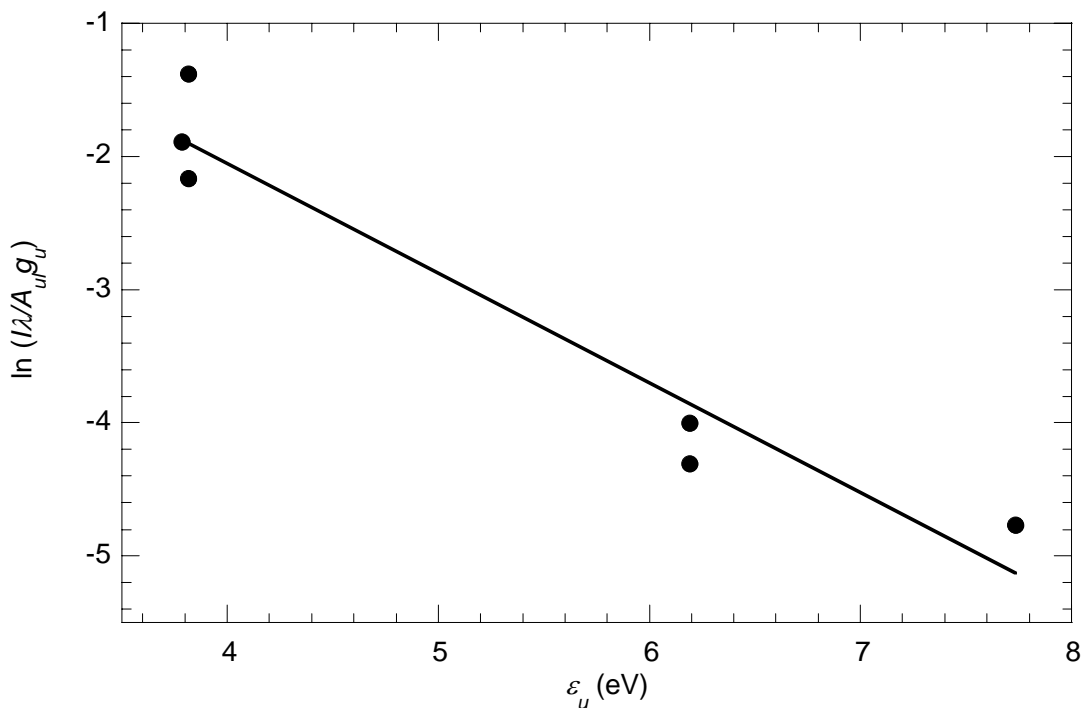


Figure 5. Boltzmann plot of Cu emission lines at 60  $\mu$ s delay; Inferred temperature 14,100 K.

There is a correlation between discharge current and measured plasma temperature as expected. Figure 6 illustrates this by comparing the temperature near the propellant surface as a function of time after discharge initiation with the absolute value of the discharge current. Because the voltage across the capillary is approximately constant, the power input is nearly proportional to the absolute value of the current. The solid line on Fig. 6 is the absolute value of the current and the symbols are the temperatures inferred from Boltzmann plots of emission intensities of *Cu* lines.

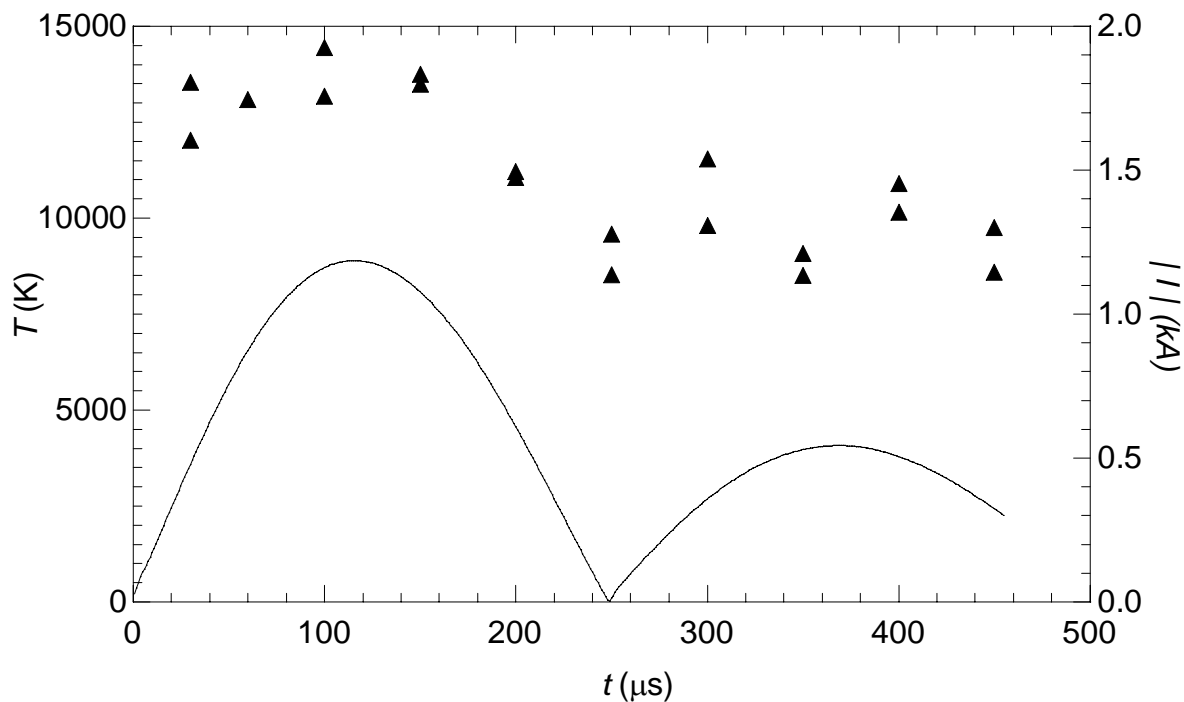


Figure 6. Variation of measured plasma temperature near propellant surface and absolute value of discharge current through capillary.

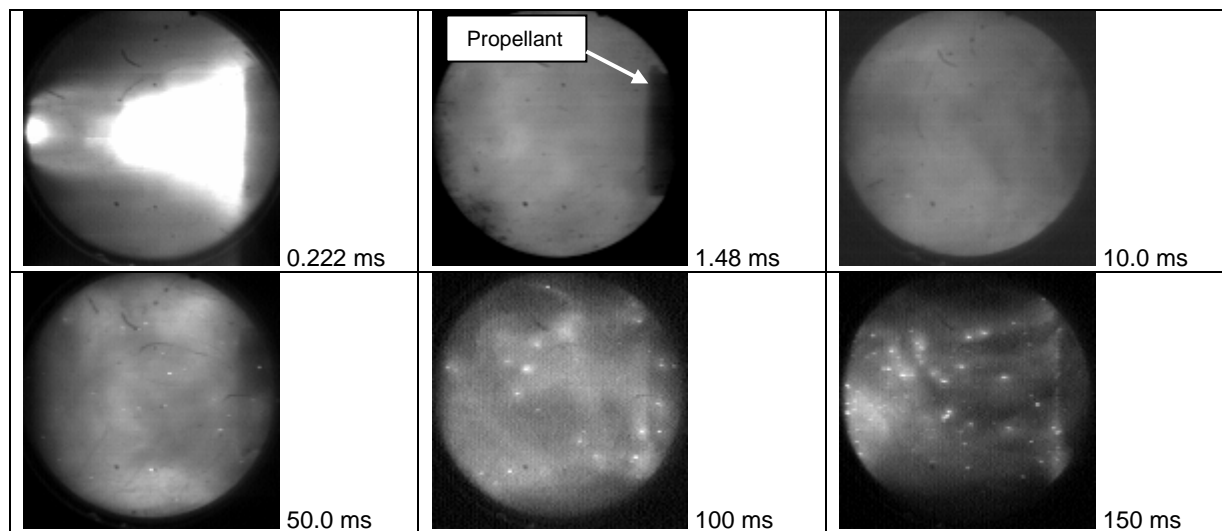


Figure 7. Visible-luminosity images of plasma-ignition of JA-2. The images were acquired at a framing rate of 13,500 frames per second.

Figure 7 shows a sequence of images of the visible luminosity for the case of plasma-ignition of JA-2 in the combustion chamber. The initial discharge voltage and energy were 4 kV and 2 kJ, respectively. These images were taken with a Kodak Ektapro HS4540 at a framing rate of 13,500 frames per second. The distance between the exit of the plasma jet and the JA-2 disk was about 20 mm. The sequence is actually a composite assembled from different runs, because a single camera/lens setting does not have sufficient dynamic range to capture the range of intensities that occur over the duration of a run. In these images the plasma axis is horizontal and it travels left to right. The propellant disk (12 mm diameter) is vertical and is labeled in the second image.

The first image, captured at 0.222 ms from the start of the plasma discharge, shows the structure of the impinging plasma jet. The luminous bore exit can be seen at left and the very luminous Mach disk is seen as the triangular shaped region at right. At this instant the propellant is enveloped in the plasma. At 1.48 ms the high plasma luminosity has largely dissipated, although swirling lower-luminosity gas can still be seen in the video images. It should also be noted that the side of the propellant mounting rod can be seen in the image. Interestingly, at 10 ms the rod is no longer visible. At between 30-50 ms the videos show bright luminous specks are ejected from the surface of the propellant, which presumably marks the beginning of ignition. Such specks can be seen at 50, 100 and 150 ms in Fig. 7.

NO<sub>2</sub> PLIF measurements have been conducted in an open air interaction between the plasma jet and propellant. An example image was shown in Fig. 2 with the plasma impinging normally on to the propellant. The image was taken at 700 μs to avoid the most intense plasma luminosity during the discharge. However, the problems associated with PLIF in the open air plasma jet can still be seen. There is still a background plasma luminosity in the image. Additionally, there is very bright laser scattering (possibly from condensing particulates) at the center of the jet leaking through the laser notch filter. There appears to be a faint fluorescent signal near the surface of the propellant but the signal quality is very poor. Because of these problems, we have built a chamber to test only a plasma radiation interaction on the propellant. Figure 8 shows the effect of plasma radiation on the surface of the propellant disks. Disk (a) is a pristine propellant disk, (b) is a disk that has been exposed to plasma radiation only, and (c) is a disk that had the plasma jet impinging directly upon it. While the level of surface reaction is noticeably less for disk (b) than (c), a large number of voids and crazes can be seen in the image. These results are consistent with other plasma radiation experiments.<sup>9</sup> We plan to make PLIF measurements of NO and NO<sub>2</sub> evolution from the propellant as a function of time during the radiation interaction.

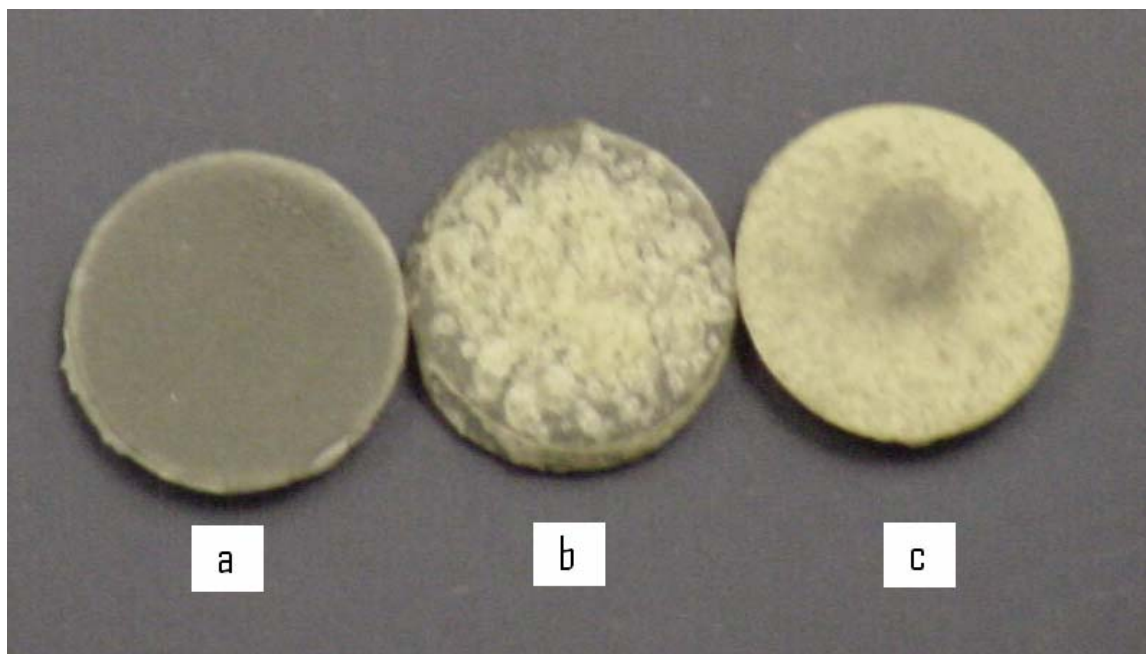


Figure 8. Propellant disks used in plasma propellant interaction: (a) pristine, (b) radiation interaction only, (c) direct plasma impingement.

## SUMMARY AND CONCLUSIONS

The work presented is part of continuing experimental study of the ignition of solid propellants by electrothermal capillary plasmas. Experiments have been made to characterize the pulsed plasma jet expanding into room air and impinging on JA-2 propellant disks. We have demonstrated that the plasma is sufficiently energetic to ignite JA-2 when the propellant disks are confined in a closed chamber. However, the formation of fine particulates due to condensation of the plasma significantly hinders the use of optical diagnostics in closed chamber experiments. Significant difficulties are present even for experiments at atmospheric pressure but PLIF measurements are feasible, especially for investigations where the propellant is only exposed to plasma radiation.

## FUTURE WORK

We plan to perform PLIF measurements on NO and NO<sub>2</sub> to quantify the effect of plasma radiation on the propellant. Additionally, we plan to use laser absorption to obtain additional information on the interaction of electrothermal plasmas with solid propellants.

## ACKNOWLEDGMENTS

This work was supported by the Army Research Office under Grant No. DAAD19-00-1-0420. The grant monitor is Dr. David Mann.

## REFERENCES

1. Z. Kaplan, D. Saphier, D. Melnik, Z. Gorelic, J. Ashkenazy, M. Sudai, D. Kimhe, M. Melnik, "Electrothermal Augmentation of a Solid Propellant Launcher," *IEEE Trans. Magnetics* **29**, Jan. 1993, p. 573.
2. Z. Kaplan, D. Melnik, M. Sudai, D. Plotnik, G. Appelbaum, D. Kimhe, R. Alimi, L. Perlmutter, "A Field Study of a Hypervelocity Solid Propellant Electrothermal 105 mm Launcher," *IEEE Trans. Magnetics* **31**, Jan. 1995, p. 425.
3. J. Greig, J. Earnhart, N. Winsor, H. McElroy, "Investigation of Plasma-Augmented Solid Propellant Interior Ballistic Processes," *IEEE Trans. Magnetics*, vol. 29, Jan. 1993, p. 555.
4. W. Oberle and K. White, "The Application of Electrothermal-Chemical (ETC) Propulsion Concepts to Reduce Propelling Charge Temperature Sensitivity," ARL-TR-1509, U.S. Army Research Laboratory, Aberdeen Proving Ground, MD, Sept. 1997.
5. R. Lieb, P. Kaste, A. Birk, A. Kinkennon, R. Pesce-Rodriguez, M. Schroeder, M. Del Guercio, "Analysis of Burning Rate Phenomena and Extinguished Solid Propellants from an Interrupted Closed Bomb with Plasma Igniter," ARL-TR-2561, U.S. Army Research Laboratory, Aberdeen Proving Ground, MD, Aug. 2001.
6. A. Koleczko, W. Ehrhardt, S. Kelzenberg, N. Eisenreich, "Plasma Ignition and Combustion," *Propellants, Explosives, Pyrotechnics* **26**, 2001, p. 75.
7. P. Kaste, A. Birk, A. Kinkennon, R. Lieb, M. Del Guercio, M. Schroeder, R. Pesce-Rodriguez, "Analysis of Burning Rate Phenomena and Extinguished Solid Propellants from an Interrupted Closed Bomb with Plasma Igniter," *IEEE Trans. Magnetics* **37** Jan. 2001, p. 173.
8. J. Kim, N.T. Clemens, P.L. Varghese, "Experimental Study of the Transient Underexpanded Jet Generated by Electrothermal Capillary Plasma," *J. Propulsion and Power* **18**, no. 6, 2002
9. R. Beyer, R. Pesce-Rodriguez, "The Response of Propellants to Plasma Radiation," ARL-TR-3189, U.S. Army Research Laboratory, Aberdeen Proving Ground, MD, June 2004.
10. K. Kappen, R. Beyer, "Progress in Understanding Plasma-Propellant Interaction," *Propellants, Explosives, Pyrotechnics* **28**, no. 1, 2003, p. 32.
11. R. A. Fifer, "Chemistry of Nitrate Ester and Nitramine Propellants," *Fundamentals of Solid-Propellant Combustion*, Progress in Astronautics and Aeronautics, v. 90, K. Kuo and M. Summerfield ed., 1984
12. J. M. Kohel, L. K. Su, N. T. Clemens, P. L. Varghese, "Emission Spectroscopic Measurements and Analysis of a Pulsed Plasma Jet," *IEEE Transactions on Magnetics* **35**, Jan. 1999, p. 201.
13. D. K. Hsu, D. L. Monts, R. N. Zare, *Spectral Atlas of Nitrogen Dioxide 5530 to 6480 Å*, Academic Press, New York, 1978.

- 
- <sup>1</sup> Z. Kaplan, D. Saphier, D. Melnik, Z. Gorelic, J. Ashkenazy, M. Sudai, D. Kimhe, M. Melnik, "Electrothermal Augmentation of a Solid Propellant Launcher," *IEEE Trans. Magnetics* **29**, Jan. 1993, p. 573.
- <sup>2</sup> Z. Kaplan, D. Melnik, M. Sudai, D. Plotnik, G Appelbaum, D. Kimhe, R. Alimi, L. Perlmutter, "A Field Study of a Hypervelocity Solid Propellant Electrothermal 105 mm Launcher," *IEEE Trans. Magnetics* **31**, Jan. 1995, p. 425.
- <sup>3</sup> J. Greig, J. Earnhart, N. Winsor, H. McElroy, "Investigation of Plasma-Augmented Solid Propellant Interior Ballistic Processes," *IEEE Trans. Magnetics*, vol. 29, Jan. 1993, p. 555.
- <sup>4</sup> W. Oberle and K. White, "The Application of Electrothermal-Chemical (ETC) Propulsion Concepts to Reduce Propelling Charge Temperature Sensitivity," ARL-TR-1509, U.S. Army Research Laboratory, Aberdeen Proving Ground, MD, Sept. 1997.
- <sup>5</sup> R. Lieb, P. Kaste, A. Birk, A. Kinkennon, R. Pesce-Rodriguez, M. Schroeder, M. Del Guercio, "Analysis of Burning Rate Phenomena and Extinguished Solid Propellants from an Interrupted Closed Bomb with Plasma Igniter," ARL-TR-2561, U.S. Army Research Laboratory, Aberdeen Proving Ground, MD, Aug. 2001.
- <sup>6</sup> A. Koleczko, W. Ehrhardt, S. Kelzenberg, N. Eisenreich, "Plasma Ignition and Combustion," *Propellants, Explosives, Pyrotechnics* **26**, 2001, p. 75.
- <sup>7</sup> P. Kaste, A. Birk, A. Kinkennon, R. Lieb, M. Del Guercio, M. Schroeder, R. Pesce-Rodriguez, "Analysis of Burning Rate Phenomena and Extinguished Solid Propellants from an Interrupted Closed Bomb with Plasma Igniter," *IEEE Trans. Magnetics* **37** Jan. 2001, p. 173.
- <sup>8</sup> J. Kim, N.T. Clemens, P.L. Varghese, "Experimental Study of the Transient Underexpanded Jet Generated by Electrothermal Capillary Plasma," *J. Propulsion and Power* **18**, no. 6, 2002
- <sup>9</sup> R. Beyer, R. Pesce-Rodriguez, "The Response of Propellants to Plasma Radiation," ARL-TR-3189, U.S. Army Research Laboratory, Aberdeen Proving Ground, MD, June 2004.
- <sup>10</sup> K. Kappen, R. Beyer, "Progress in Understanding Plasma-Propellant Interaction," *Propellants, Explosives, Pyrotechnics* **28**, no. 1, 2003, p. 32.
- <sup>11</sup> R. A. Fifer, "Chemistry of Nitrate Ester and Nitramine Propellants," Fundamentals of Solid-Propellant Combustion, Progress in Astronautics and Aeronautics, v. 90, K. Kuo and M. Summerfield ed., 1984
- <sup>12</sup> J. M. Kohel, L. K. Su, N. T. Clemens, P. L. Varghese, "Emission Spectroscopic Measurements and Analysis of a Pulsed Plasma Jet," *IEEE Transactions on Magnetics* **35**, Jan. 1999, p. 201.
- <sup>13</sup> D. K. Hsu, D. L. Monts, R. N. Zare, *Spectral Atlas of Nitrogen Dioxide 5530 to 6480 Å*, Academic Press, New York, 1978.

# Spectroscopic Measurements During an Electrothermal Plasma-JA2 Solid Propellant Interaction

Michael D. Ryan,<sup>\*</sup> Noel T. Clemens,<sup>†</sup> and Philip L. Varghese<sup>‡</sup>  
*Center for Aeromechanics Research,  
The University of Texas at Austin, Austin, Texas 78712-1085*

A variety of planar laser diagnostics were conducted on reaction products resulting from the interaction between radiation from an electrothermal plasma and JA2 solid propellant. JA2 discs were exposed to radiation from a confined 3.1 kJ electrothermal plasma discharge. The induced reactions in the propellant surface produce decomposition products as well as particulates that escape the propellant and propagate away from the surface. Nitric oxide (NO) is a common double base propellant decomposition product. Planar laser induced fluorescence (PLIF) measurements of NO were made in the gas bordering the propellant during the 600  $\mu$ s plasma discharge. Also, planar laser scattering (PLS) was conducted on the particulates in that same region. No reaction products were observed for the first 100  $\mu$ s after the discharge was triggered. Clouds of NO and scattering particles appeared at the propellant surface after this 100  $\mu$ s delay and expanded and propagated away from the surface as the discharge progressed. The clouds appeared in two varieties, the more prevalent type characterized by lower fluorescence and scattering signals with a globular structure, and the rarer type characterized by a larger size, very bright scattering signals, brighter fluorescence, and a smoother surface.

## I. Introduction

Electrothermal plasma ignition of solid propellants has been studied for the last 15 years for the purposes of implementation into tanks guns. Electrothermal plasmas are produced through the ablation and ionization of material inside plastic capillaries through which large capacitors are discharged. The original objective of plasma ignition was to increase muzzle velocity over conventional ignition. However, without a prohibitively large plasma energy input, it has been shown that the only way to increase muzzle velocity is for the plasma to increase the burn rate of the propellant.<sup>1</sup> Unexpected benefits of plasma ignition were a reduction in ignition delay and delay jitter over conventional ignition<sup>2</sup> as well temperature compensation for the propellant.<sup>3</sup> These benefits increase gun accuracy over a range of environmental conditions. There is no consensus as to what attributes of the plasma actually drive the ignition and hence cause these benefits. Possibilities include metallic vapor deposition onto the propellant, increased heat flux from the hot plasma, higher reactivity of the plasma from ionized species, or higher radiative flux into the propellant from the plasma.

It has been proposed that in depth radiation effects on transparent propellants (M9 and graphite-free JA2) and semi-transparent propellants (JA2) cause the formation of surface blisters and in-depth voids which provide increased surface area for gasification during the plasma discharge.<sup>4</sup> Because propellant burning rate is strongly dependent on pressure, this gasification and subsequent increased pressure rise early in the ignition is what causes the reduction in ignition delay and jitter. Other work shows that the gases created solely by radiative decomposition can be significant.<sup>5</sup> In addition, it has been shown that propellant burning rate can be increased if blisters and voids are created to significant depth in transparent JA2.<sup>6</sup>

There is a significant amount of literature on radiative<sup>7,8</sup> and thermal<sup>9-11</sup> decomposition of propellants, radiative ignition<sup>12-14</sup> of propellants as well as a few studies on propellant effects induced by plasma radiation. While some deal with the chemical species involved, none deal with transport of species in the fluid surrounding the propellant for this important precursor to ignition. Previous studies of plasma radiation-propellant interactions analyzed propellant composition or induced gas composition after the plasma firing.<sup>5</sup> The experiments described here were

---

<sup>\*</sup> Graduate Student, ASE-EM Dept.

<sup>†</sup> Professor, ASE-EM Dept., Associate Fellow AIAA

<sup>‡</sup> Professor, ASE-EM Dept., Associate Fellow AIAA

designed to provide temporally and spatially resolved species information during the plasma radiation-propellant interaction.

## II. Experimental Setup

### A. Plasma Radiation Chamber

The apparatus used to create the electrothermal plasma has been described previously<sup>15,16</sup> and is briefly described here. A 251  $\mu\text{F}$  capacitor charged to 5 kV connects to the discharging circuit via an ignitron mercury vapor switch. Once triggered, and after a few microsecond delay, current conducts from the capacitor to a 25  $\mu\text{H}$  inductor along coaxial cables. Traveling from the inductor and through a copper-tungsten alloy nipple inserted in the bottom of a polycarbonate capillary (3 mm dia. by 30 mm), the current explodes a 51  $\mu\text{m}$  copper fuse wire running the length of the capillary bore. The wire explodes in the first 20  $\mu\text{s}$  of the discharge which is sustained by ablation and ionization of material from the capillary surface. Current exits through an annular electrode at the top of the capillary serving as a nozzle for the plasma jet and is conducted to ground via the metal capillary enclosure and the same coaxial cables described above. The plasma discharge into the radiation chamber lasts around 600  $\mu\text{s}$  and the total energy stored in the capacitor before the discharge is 3.1 kJ.

The plasma does not make direct contact with the propellant surface in these experiments; only radiation from the plasma impinges on the propellant surface. In all the experiments in this study a chamber was bolted onto the plasma producing device in order to increase the residence time and possibly the density of the plasma in front of the propellant. Both of these effects would cause an increase of radiative energy transferred to the surface of the propellant relative to an open air discharge. In order to minimize the metal deposition inside the chamber and the capillary, a 3 mm diameter exhaust vent was drilled through the side of the chamber for the plasma to exhaust. While the plasma was not completely confined, the capacitor discharge did last up to 100  $\mu\text{s}$  longer than during a discharge into open air.

Figure 1 shows the setup of the capillary enclosure along with the plasma chamber for a typical laser diagnostics experiment for a plasma radiation-propellant interaction. A 1.27 cm diameter disk of JA2 propellant (0.05% graphite by weight) punched from a 2.54 mm sheet is fastened to the bottom of a steel rod above the chamber window before each firing. The side surface facing the camera is coated with a lamp black solution to minimize the luminosity from the propellant and to better see signal just below the surface. The bottom surface of the propellant is 2.70 cm from the edge of the plasma chamber.

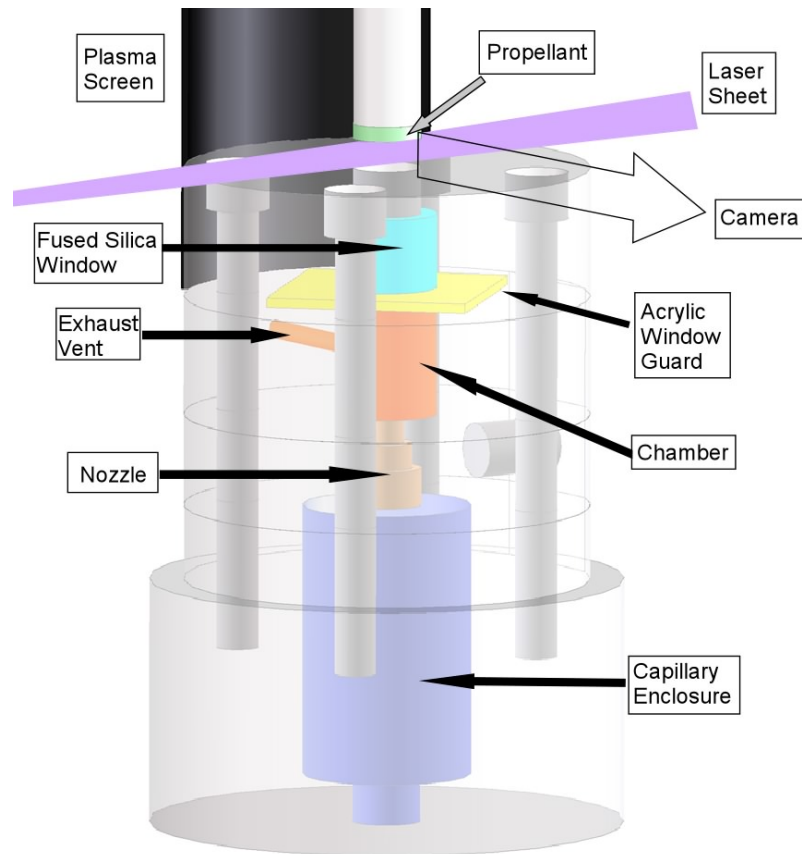


**Figure 1. Capillary enclosure and discharge chamber with window for**

The plasma is produced inside the capillary, propagates through the nozzle, and then expands into the chamber (5.8  $\text{cm}^3$ ). The plasma is completely isolated from the propellant except for a 1.27 cm thick fused silica window on

the top of the chamber protected by a 1.59 mm thick disposable clear acrylic sheet. Plasma radiation encompassing the visible spectrum to below 380 nm propagates through the window and causes reactions in the propellant while the capacitor is discharging and as the plasma exhausts through the vent for a few hundred microseconds after the discharge. To reduce background light a blackened aluminum foil screen attached to the chamber wall blocks the camera's view of the plasma exhaust.

Two data sets were taken to qualify the plasma radiation through the chamber window. The radiation intensity time history during a firing was measured using a fast response photodiode put in place of the propellant with an ND 200 filter attenuating the light. Also, the emission spectrum was measured at two different times during the discharge. A fused silica lens focused plasma light onto a 100  $\mu\text{m}$  fiber optic which a Spex 1681 spectrograph spectrally resolved (50  $\mu\text{m}$  slit width) and a Roper Scientific PI-Max intensified CCD camera recorded. The camera was gated to 1  $\mu\text{s}$  and only one spectrum was taken per firing because image acquisition speed was much slower than 600  $\mu\text{s}$ . However, the spectra were repeatable enough that multiple spectra taken over different spectral ranges at a given delay could be spliced together to form an emission curve.

## B. Laser Diagnostics

Figure 2 shows the experimental setup for the NO PLIF experiment. There are a few steps involved to create the  $\sim 226$  nm light needed to pump NO. A frequency doubled Spectra Physics GCR 150 Nd:YAG 10 Hz pulsed laser at 532 nm is used to pump a Lumonics HyperDye-300 laser. The dye laser with a  $2 \cdot 10^{-4}$  molar concentration of Pyromethene 597 in ethanol is tuned to output a  $\sim 574$  nm beam which is then frequency doubled with a KDP crystal inside an Inrad Autotracker II. The resulting  $\sim 287$  nm light is combined with the residual 1064 nm light from the Nd:YAG that has been time delayed to coincide with the dye beam by lengthening the laser path across the table. The combined beams are then mixed in a KDP crystal inside a second Inrad Autotracker II to create the  $\sim 226$  nm beam. This beam is separated from the residual 1064 and doubled dye beams with a Pellin Broca prism which also steers it to the plasma chamber. The  $\sim 1$  mJ laser is focused with a 1 m focal length fused silica lens and then expanded into a sheet using a 25.4 mm focal length cylindrical lens. The cylindrical lens is placed only a few inches from the propellant because the field of view is only 5 mm tall. The cylindrical lens is not burned because of the lower power of the  $\sim 226$  nm beam.

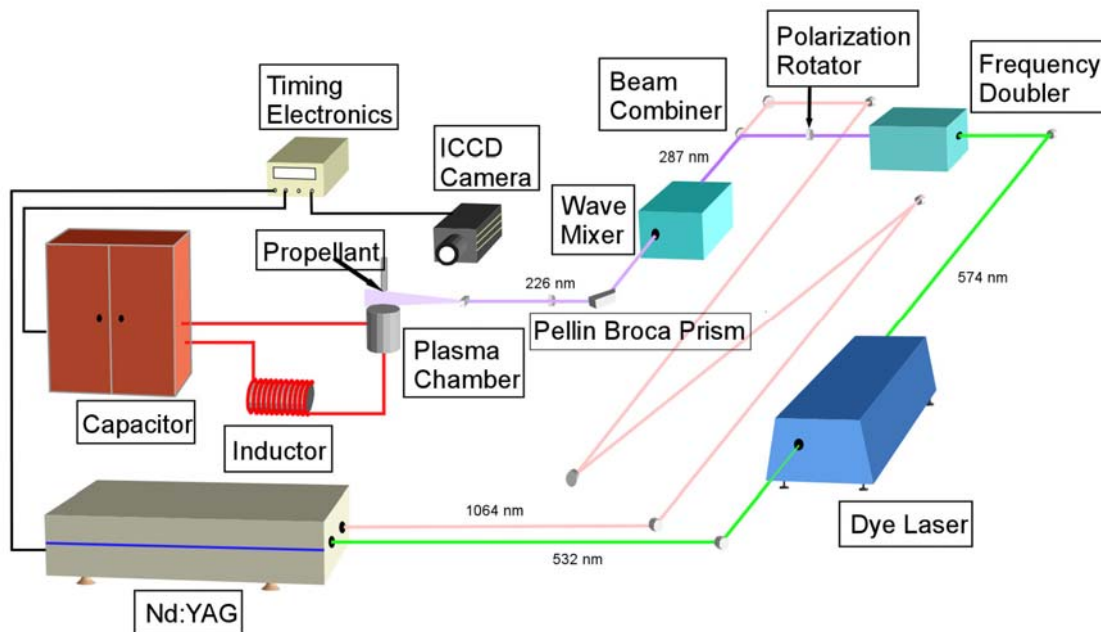


**Figure 2. NO PLIF experimental setup**

Because the fluorescence experiment was only qualitative in nature, exploring where and when NO was present in the flow, it was only necessary to tune the dye laser wavelength to a strong absorption line without worrying

about fluorescence mechanics. The first excited electronic transition of NO,  $A^2\Sigma^+(v'=0) \leftarrow X^2\Pi(v''=0)$  was employed for fluorescence imaging. The laser was calibrated using a test cell filled with 25 ppm NO in  $N_2$  at atmospheric pressure. The laser was scanned across the absorption lines of the first excited electronic transition of NO and the broadband fluorescence signal was collected through a UG5 filter on a Hamamatsu PMT. An SRS 250 Boxcar Averager/Gated Integrator was used to collect fluorescence signal synchronous with the laser pulses. This absorption spectrum was matched to a calculated spectrum<sup>17</sup> and the  $Q_{21}+R_{11}(9.5)$  transition pair at 225.9802 nm was the pumped for the PLIF measurements.

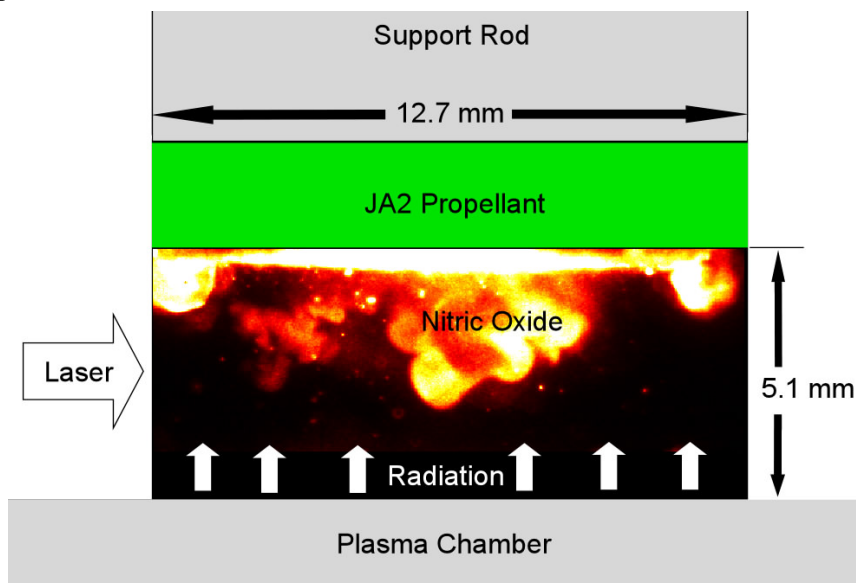


**Figure 3. Geometry for camera field of view in all laser diagnostic experiments**

Fluorescence imaging was conducted using a Roper Scientific PI-Max 512 intensified CCD camera. A UG-5 UV filter was placed in front of the Nikor Nikon UV lens to attenuate laser light scatter onto the CCD. The field of view geometry can be seen in Fig. 3. The propellant surface at the top of the image is 12.7 mm wide. It is 5 mm from the top surface of the plasma chamber, which is cropped from the bottom of the image. The propellant surface is never exactly flat and changes over time during the interaction as material is

blown off the surface. An example NO PLIF image can be seen in Fig. 3 where the brightest swath at the top of the image is actually propellant luminosity/radiation scattering. All timing was run off a 10 Hz signal from a BNC signal generator. An in house trigger box was used to synchronize the plasma firing and camera acquisition to the laser pulse appropriately delayed by SRS delay generators. Because the laser pulse period and camera readout time was much longer than the plasma discharge time of 600  $\mu s$ , only one image was taken per firing. A series of NO fluorescence images were taken from 100  $\mu s$  delay from the plasma trigger (when NO first began to appear) to 600  $\mu s$  (when the capacitor finished discharging) at 50  $\mu s$  time intervals. Usually two to three images were taken at each time delay, but only one set is shown in this paper. While NO was present after 600  $\mu s$ , we were not interested in dissipation of the NO after the plasma because in a real plasma ignition event NO would be produced continuously until ignition.

In addition to NO fluorescence, two other laser diagnostic imaging experiments were conducted. The first was PLIF of  $NO_2$ , one of the first decomposition products of a nitrate ester propellant.  $NO_2$  has a broadband visible absorption spectrum with four electronic states directly or indirectly interacting along with a complicated vibrational and rotational band structure.<sup>18</sup> This qualitative experiment was once again designed to record the time and place of any  $NO_2$  in the flow.  $NO_2$  was pumped using the same frequency doubled Spectra Physics Nd:YAG at 532 nm mentioned previously. The ~100 mJ per pulse laser was apertured to 5 mm high and formed into a sheet by a 225 mm convex cylindrical lens. The broadband fluorescence was imaged with the PI-Max ICCD through an OG-570 color glass filter to cut out laser scattering. The setup was the same as in Fig. 1, with the only difference being the pump laser.

While conducting the fluorescence experiments, a small amount of scattering off large particles was seen throughout the flow. This warranted further study and a scattering experiment using the frequency doubled Nd:YAG was conducted. The same intensified CCD camera was used, this time looking through OG 515 and BG 38 filters to attenuate luminosity from the propellant surface. The laser, this time at ~20 mJ/pulse, was formed into a sheet by the same method as in the  $NO_2$  experiment.

### III. Results and Discussion

#### A. Plasma Radiation

Figure 4 shows the plasma radiation intensity measured by the fast response photodiode. The intensity ramps up very fast and peaks at around 80  $\mu$ s. Afterwards the radiation has a steady decline until between 600-650  $\mu$ s, when the capacitor stops discharging. After that it seems that the intensity decays exponentially. The reason for the dip in intensity around 300  $\mu$ s is unknown. After the firing the acrylic window guard is always somewhat blackened and the surface looks like it was partially melted from deposition from the plasma. The steady intensity decay during the discharge might be explained by the effect of the plasma on the acrylic sheet. We were unable to make radiative heat flux measurements to the surface of the propellant, but for an order of magnitude estimate it can be assumed the confined plasma produces flux equal to or higher than the same plasma expanding into open air. The peak radiative flux on a probe 4.67 cm from the jet exit of a plasma expanding into room air was measured at 2500 W/cm<sup>2</sup> and the flux was above 1000 W/cm<sup>2</sup> for the entire capacitor discharge.<sup>19</sup>

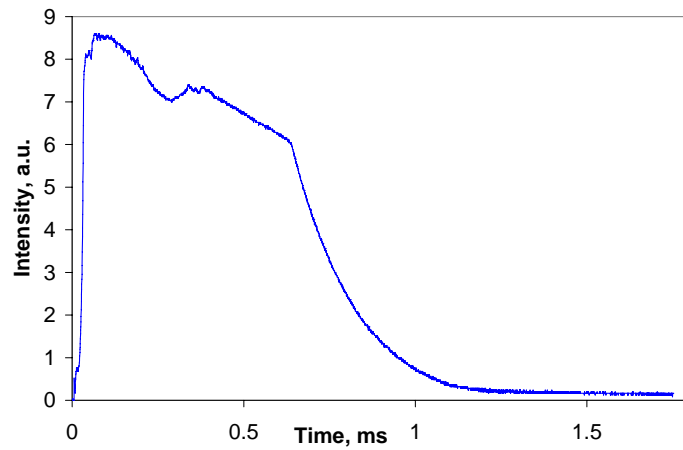


**Figure 4. Plasma radiation intensity measured by a fast response photodiode**

Plasma spectra combined from a number of firings can be seen in Fig. 5. The spectral range of the spectrometer is 120 nm so each curve is a combination of 4 acquisitions at the same delay. Curves were produced for 150  $\mu$ s and 500  $\mu$ s delays. At both delays the spectrum is characterized by broadband emission with a few noticeable absorption lines or bands at 428, 470 and 520 nm. This is characteristic of a confined electrothermal plasma discharge. The cutoff below 380 nm is due to attenuation by acrylic. The oscillations on the right side of both curves are due to interference fringes on the detector. The emission intensity at 500  $\mu$ s is much less than that at 150  $\mu$ s and the spectrum changes over time. At 150  $\mu$ s there is a marked peak at 400 nm, while at 500  $\mu$ s the peak seems to have shifted to between 500-600 nm. Because the acrylic cuts off at 380 nm, it is impossible to know where the true plasma radiation peak is. Also, because optical quality of the acrylic degrades over time in the chamber, it is difficult to say if the changes in the spectra are due to changes in the plasma light source or in the transmittance of the acrylic.

Before these radiation experiments began there was some question as to how much our plasma radiation would affect the propellant, and also how similar the effects would be to other studies that focus on graphite free JA2 interactions.<sup>5,6</sup> Most tests involving plasma propellant interactions involve higher plasma energies than the 3.1 kJ that our setup uses. In addition, graphite free JA2 transmits more radiation in depth than the propellant used in these experiments. Figure 6 shows a propellant disc before and after exposure to plasma radiation. The level of interaction, while not as great as when a plasma jet impinges on the propellant in open air, and far from ignition, is enough to have clear visible effects on the surface of the JA2 disc. The “bubble like” features shown in the previously referenced papers are similar if not the same structures seen on the surface of this propellant.

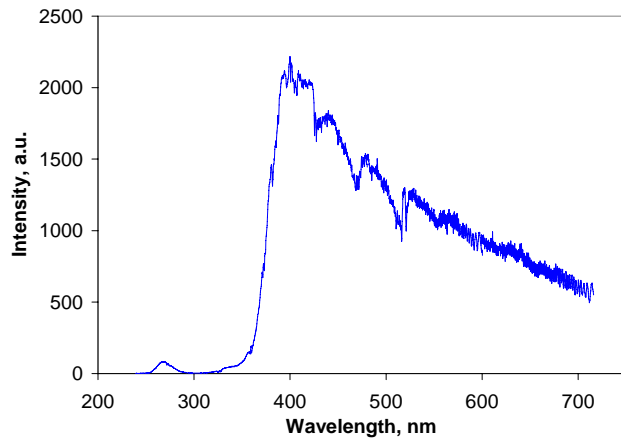
#### B. NO PLIF

A series of example NO PLIF images, one taken from each delay sampled, can be seen in Fig. 7. They are arranged such that a representative time history is shown. Each image is false colored from grayscale and has been rescaled individually in order to better visualize the NO. Many of the images show scattering off large particles as well as bright structures related to the disc edge in addition to the structures containing NO below the center of the propellant that seem to be related to the crazes and voids observed on the propellant surface after the firing. To distinguish between NO fluorescence and scattering, a few images were taken with the pump laser tuned slightly off resonance. An example image at 500  $\mu$ s delay can be seen in Fig. 8. This image was scaled such that signal of the same intensity as the minimum brightness structures in the NO PLIF images would clearly be visible. The large particles can still be seen in Fig. 8 as well as some signal very close to the propellant surface. However, nothing resembling the large structures either below the propellant surface or at the edge is observed.

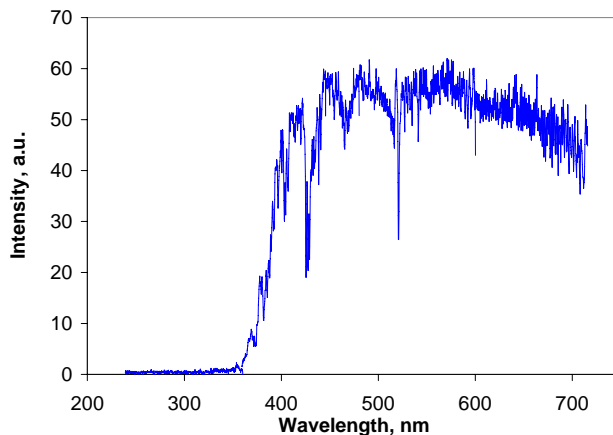
NO signal is not observed until after 100  $\mu$ s. At 150  $\mu$ s small globular clouds appear and grow as the discharge progresses. In many of the images, especially at times after 350  $\mu$ s, discrete nitric oxide clouds can be seen separate from the propellant surface. This suggests that NO is being produced in short bursts rather than continuous jets during the discharge. An alternative, though less likely explanation, is that the clouds of NO propagate parallel to the surface of the propellant. From the original images it can be inferred that the brightest NO signal is present when the clouds first appear at 150  $\mu$ s, and the signal gradually decreases until 300  $\mu$ s where it stays relatively constant. The temperature at the propellant surface and the gases being released by the propellant during the interaction was not

measured. Calculated spectra show that signal should decrease with increasing temperature. It would be reasonable to assume that the change in maximum signal is driven by the change in NO concentration because the highest temperature would be expected when the NO escapes from the propellant and that is where the highest signals are seen.

Velocity of the NO clouds was roughly estimated by measuring the average rate of change of the distance from the bottom edge of the clouds to the propellant surface. The order of magnitude of the velocity calculated was 10 m/s. The pressure difference between the surface of the propellant and the atmosphere needed to cause this velocity is only a small fraction of atmospheric pressure. While double base propellant decomposition can be pressure dependent due to autocatalysis from NO<sub>2</sub>,<sup>20</sup> pressures changes in these experiments are insignificant.



a)



b)

**Figure 5. Plasma emission spectra at a) 150  $\mu$ s b) 500  $\mu$ s**

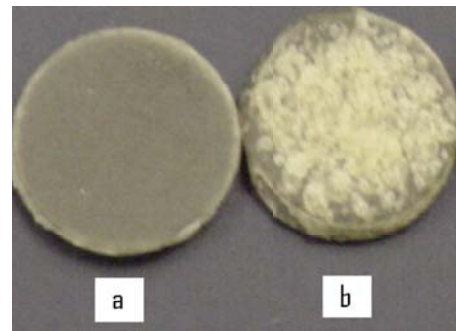


**Figure 6. JA2 disc surface a) before and b) after plasma radiation exposure**

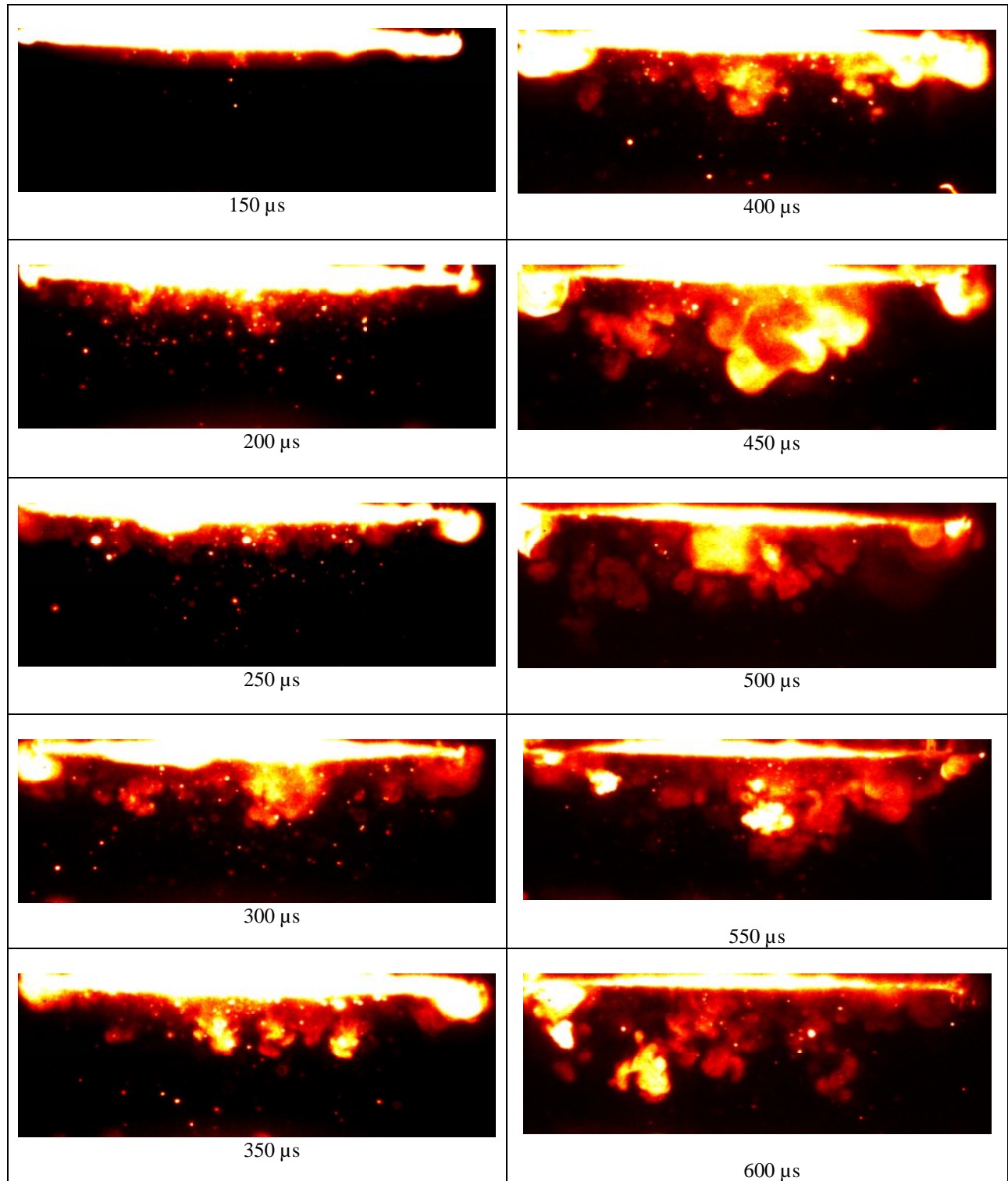


**Figure 7. Time sequence of NO PLIF images created from separate firings**

### C. NO<sub>2</sub> PLIF and Laser Scattering Imaging

NO<sub>2</sub> was not detected at all during the plasma propellant radiation interaction. Figure 9 shows an example NO<sub>2</sub> PLIF image taken at 200  $\mu$ s. Scattering of large particles, as well as probable scattering from edge structures can be seen in the image. Also, the bulbous structure in the center at the propellant surface is most likely scattering as well. The intensity is nearly the same as the rest of the surface and PLIF signal was expect to be weak. NO<sub>2</sub> was unlikely to be observed because it is a broadband absorber and it usually quickly dissociates into NO during nitrate ester decomposition in atmospheric pressure air.<sup>21</sup>

Figure 10 shows laser scattering images taken with the same laser (at lower power) and different filters for the camera. These were also individually rescaled and false colored from grayscale images. A representative time history similar to Fig. 7 gives an idea of the type of scattering structures and how they propagate during the discharge. Once again the structures begin to appear at 150  $\mu$ s and grow larger and propagate down as the discharge progresses. There seems to be two types of distinct scattering structures. The first, composed of a range of particle sizes, seem to appear and grow as the large majority of NO clouds do in Fig. 7. The shapes are similar enough that they probably are the same structures. The second, seen only in the 400 and 450  $\mu$ s images below the propellant, but also throughout the images at the edge, is characterized by much brighter scattering and homogeneity of the particle sizes, inferred from the relatively constant signal throughout the structure. This structure type was much rarer, as it was only seen on those two images in all the runs. However, the surface of the propellant after these two runs looked no different to the naked eye than after any other run. A corresponding NO cloud might be seen in the 450  $\mu$ s image of Fig. 7. The large NO cloud in the center of that image is brighter than the surrounding clouds, bigger, and has a much smoother surface.

The images show a large amount of particulates separating from the propellant surface during the radiation interaction. The particulates have a range of sizes. Because JA2 propellant has three major nitrate esters, two of which are liquid at room temperature nitroglycerin (NG) and diethylene glycol dinitrate (DEGDN), and many other components at low concentration, it is impossible to know what the composition of the particles are in the images. They could be chunks of nitrocellulose (NC) fiber, liquid mists of NG or DEGDN, an agglomeration of NC, NG, and DEGDN, or some smaller decomposition product that scatters light. The large jump in pressurization seen in closed bomb plasma ignition tests<sup>22</sup> during the plasma discharge might be due in part to the increased burning surface area provided by these particles, in addition to the known outgassing that occurs. No films or buildup of particulates was ever observed on the top of the chamber. For an individual firing the particulates are either a small amount of material, or they evaporate by the end of the run.

The structures observed jetting from the propellant could directly correspond to individual blister formation on the propellant surface. Blisters overlap on the propellant surface so clear individual jets would not be expected during the discharge. The images shown in this work are not correlated with any surface effects at this point, but hopefully work planned for the future will show this correspondence.

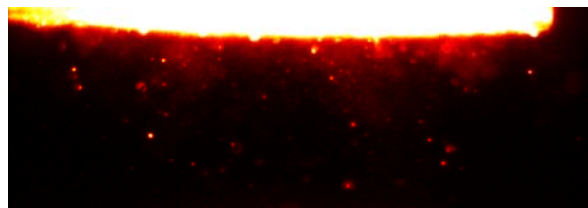


**Figure 8. Example image of tuning NO pump laser off absorption line at 500  $\mu$ s delay**



**Figure 9. Example NO<sub>2</sub> PLIF image at 200  $\mu$ s**

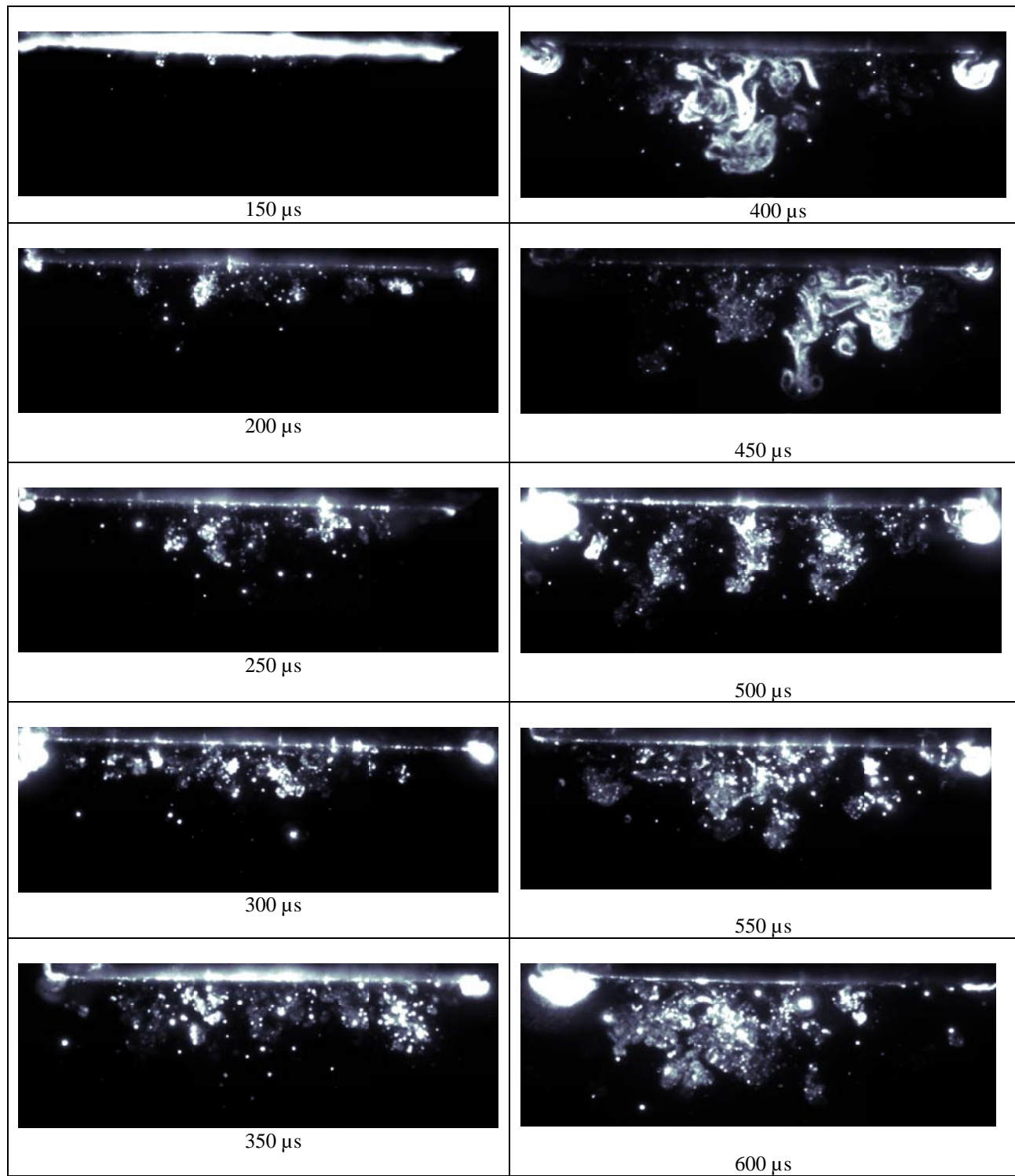


**Figure 10. Time sequence of Nd:YAG scattering images created from separate firings**

#### IV. Conclusion

Quantitative measurements of the interaction between an electrothermal plasma and propellant are challenging. In this paper we have presented space- and time-resolved measurements that show the spatial and temporal scales of the evolution of a propellant decomposition product (NO) and ejected particulates as the propellant responds to intense radiation from the plasma. The jet structures observed that contain both NO and scattering particles probably correspond to individual blister formation in the propellant.

In order to characterize the interaction more completely, one would need to correlate ejected gas structures with propellant surface changes during the discharge. Also time-resolved measurements of the propellant temperature, and also measurements of the temperature of the evolved NO would be useful. The gas temperature measurement would also permit a quantitative estimate of NO concentration. Work is in progress to address these issues.

#### Acknowledgments

This work was supported by the Army Research Office under Grant No. DAAD19-00-1-0420. The grant monitor was Dr. David Mann.

#### References

1. White, K., Stobie, I., Oberle, W., Katulka, G., Driesen, S., "Combustion Control Requirements in High Loading Density, Solid Propellant ETC Gun Firings," *IEEE Transactions on Magnetics* **33**, Jan. 1997, p. 350.
2. Taylor, M., "Ignition of Propellant by Metallic Vapour Deposition for an ETC Gun System," *Propellants, Explosives, Pyrotechnics* **26**, 2001, p. 137.
3. Oberle, W., White, K., "The Application of Electrothermal-Chemical (ETC) Propulsion Concepts to Reduce Propelling Charge Temperature Sensitivity," ARL-TR-1509, U.S. Army Research Laboratory, Aberdeen Proving Ground, MD, Sept. 1997.
4. Pesce-Rodriguez, R.A., and Beyer, R.A., "A Theory of Plasma-Propellant Interactions," ARL-TR-3286, U.S. Army Research Laboratory, Aberdeen Proving Ground, MD, Sept. 2004.
5. Beyer, R., Pesce-Rodriguez, R., "The Response of Propellants to Plasma Radiation," ARL-TR-3189, U.S. Army Research Laboratory, Aberdeen Proving Ground, MD, June 2004.
6. Koleczko, A., Ehrhardt, W., Kelzenberg, S., Eisenreich, N., "Plasma Ignition and Combustion," *Propellants, Explosives, Pyrotechnics* **26**, 2001, p. 75.
7. Clark, D.T., Stephenson, P.J., "An ESCA Study of the Surface Chemistry of Cellulose Nitrates and Double Based Propellants, with Particular Reference to their Degradation in Ultra-Violet Light," *Polymer Degradation and Stability* **4**, 1982, pp. 185-193.
8. Yang, M., Ramsy, J.M., and Kim, B.J., "Laser-induced Selective Dissociation of Nitro Groups in Nitrocellulose," *Rapid Communications in Mass Spectrometry* **10**, 1996, pp. 311-315.
9. Kucera, V. and Havrankova, E., "Investigation of the Decomposition Processes in Double-Base Propellants and Nitrocellulose under Vacuum and Oxygen," *Propellants, Explosives, Pyrotechnics* **13**, 1988, pp. 186-188.
10. Kimura, J., "Chemiluminescence Study on Thermal Decomposition of Nitrate Esters (PETN and NC)," *Propellants, Explosives, Pyrotechnics* **14**, 1989, pp. 89-92.
11. Roos, B.D. and Brill, T.B., "Thermal Decomposition of Energetic Materials 82. Correlations of Gaseous Products with the Composition of Aliphatic Nitrate Esters," *Combustion and Flame* **128**, 2002, pp. 181-190.
12. DeLuca, L., Caveny, L.H., Ohlemiller, T.J., and Summerfield, M., "Radiative Ignition of Double-Base Propellants: I. Some Formulation Effects," AIAA 11th Aerospace Sciences Meeting, Washington, D.C., Jan. 1973.
13. Ahmad, S.R. and Russell, D.A., "Studies into Laser Ignition of Unconfined Propellants," *Propellants, Explosives, Pyrotechnics* **26**, 2001, pp. 235-245.
14. Weber, J.W., Brewster, M.Q., and Tang, K.C., "Radiative Ignition and Extinction Dynamics of Energetic Solids," *AIAA J. Thermophysics and Heat Transfer* **19**, n. 3, 2005, p. 257.
15. Kohel, J. M., Su, L. K., Clemens, N. T. and Varghese, P. L., "Emission Spectroscopic Measurements and Analysis of a Pulsed Plasma Jet," *IEEE Transactions on Magnetics* **35** (1), 1999, pp. 201-206.
16. Kim, J. U., Clemens, N.T. and Varghese, P.L., "Experimental Study of the Transient Underexpanded Jet Generated by an Electrothermal Capillary Plasma," *AIAA J. Propulsion and Power* **18** (6), 2002, pp. 1153-1160.
17. Seitzman, Jerry M., "Lines," "Spectra," Version 3.0, High Temperature Gasdynamics Laboratory, Mech. Engin. Dept., Stanford University, ©1985-1990.
18. Hsu, D. K., Monts, D. L., Zare, R. N., *Spectral Atlas of Nitrogen Dioxide 5530 to 6480 Å*, Academic Press, New York, 1978.
19. Ryan, M.D., Clemens, N.T., Varghese, P.L., "Measurements of Electrothermal-Plasma Ignition of Solid Propellants," AIAA-2004-0388, AIAA 42nd Aerospace Sciences Meeting and Exhibit, 2004.
20. Kimura, J., "Kinetic Mechanism on Thermal Degradation of a Nitrate Ester Propellant," *Propellants, Explosives and Pyrotechnics* **13**, 1988, p. 8.

21. Oyumi, Y., and Brill, T.B., "Thermal Decomposition of Energetic Materials 14. Selective Product Distributions Evidenced in Rapid, Real-Time Thermolysis of Nitrate Esters at Various Pressures." *Combustion and Flame* **66**, 1986, pp. 9-16.
22. Lieb, R.J., Kaste, P.J., Birk, A., Kinkennon, A., Pesce-Rodriguez, R.A., Schroeder, M.A., and Del Guercio, M., "Analysis of Burning Rate Phenomena and Extinguished Solid Propellants From an Interrupted Closed Bomb with Plasma Igniter," ARL-TR-2561, U.S. Army Research Laboratory, Aberdeen Proving Ground, MD, August 2001.